Langerhans cell function: enhanced contact hypersensitivity responses in OX40L-transgenic mice. Eur J Immunol 2002;32:3326.
[19] Fillatreau S, Gray D. T-cell accumulation in B cell follicles is regulated by dendritic cells and is independent of B cell activation. J Exp Med 2003;197:195.
[20] Ito T, Amakawa R, Inaba M, Hori T, Ota M, Nakamura K, Takebayashi M, Miyaji M, Yoshimura T, Inaba K, Fukuhara S. Plasmacytoid dendritic cells regulate Th cell responses through OX40 ligand and type I IFNs. J Immunol 2004;172:4253.
[21] Zingoni A, Sornasse T, Cocks BG, Tanaka Y, Santoni A, Lanier LL. Cross-talk between activated human NK cells and CD4 T cells via OX40-OX40 ligand interactions. J Immunol 2004;173: 3716.
[22] Kashiwakura J, Yokoi H, Saito H, Okayama Y. T-cell proliferation by direct cross-talk between OX40 ligand on human mast cells and OX40 on human T cells: comparison of gene expression profiles between human tonsillar and lung-cultured mast cells. J Immunol 2004;173:5247.
[23] Mestas J, Crampton SP, Hori T, Hughes CC. Endothelial cell co-stimulation through OX40 augments and prolongs T-cell cytokine synthesis by stabilization of cytokine mRNA. Int Immunol 2005;17:737.
[24] Compaan DM, Hymowitz SG. The crystal structure of the costimulatory OX40-OX40L complex. Structure 2006;14:1321.
[25] Takasawa N, Ishii N, Higashimura N, Murata K, Tanaka Y, Nakamura M, Sasaki T, Sugamura K. Expression of gp34 (OX40 ligand) and OX40 on human T-cell clones. Jpn J Cancer Res 2001;92:377.
[26] Tanaka Y, Inoi T, Tozawa H, Yamamoto N, Hinuma Y. A glycoprotein antigen detected with new monoclonal antibodies on the surface of human lymphocytes infected with human T-cell leukemia virus type-I (HTLV-I). Int J Cancer 1985;36:549.
[27] Kim MY, Bekiraris V, McConnell FM, Gaspal FM, Raykundalia C, Lane PJ. OX40 signals during priming on dendritic cells inhibit CD4 T-cell proliferation: IL-4 switches off OX40 signals enabling rapid proliferation of Th2 effectors. J Immunol 2005;174:1433.
[28] Mendel I, Shevach EM. Activated T cells express the OX40 ligand: requirements for induction and costimulatory function. Immunology 2006;117:196.
[29] Soroosh P, Ine S, Sugamura K, Ishii N. OX40-OX40 ligand interaction through T cell-T-cell contact contributes to CD4 T-cell longevity. J Immunol 2006;176:5975.
[30] Tozawa H, Andoh S, Takayama Y, Tanaka Y, Lee B, Nakamura H, Hayami M, Hinuma Y. Species-dependent antigenicity of the 34-kDa glycoprotein found on the membrane of various primate lymphocytes transformed by human T-cell leukemia virus type-I (HTLV-I) and simian T-cell leukemia virus (STLV-I). Int J Cancer 1988;41:231.
[31] Inudoh M, Kato N, Tanaka Y. New monoclonal antibodies against a recombinant second envelope protein of hepatitis C virus. Microbiol Immunol 1998;42:875.
[32] Takahashi Y, Tanaka Y, Yamashita A, Koyanagi Y, Nakamura M, Yamamoto N. OX40 stimulation by gp34/OX40 ligand enhances productive human immunodeficiency virus type 1 infection. J Virol 2001;75:6748.
[33] Tanaka Y, Yoshida A, Tozawa H, Shida H, Nyunoya H, Shimotohno K. Production of a recombinant human T-cell leukemia virus type-1 trans-activator(tax1) antigen and its utilization of monoclonal antibodies against various epitopes on the tax1 antigen. Int J Cancer 1991;48:623.
[34] Kim MY, Anderson G, White A, Jenkinson E, Arlt W, Martensson IL, Erlandsson L, Lane PJ. OX40 ligand and CD30 ligand are expressed on adult but not neonatal CD4 CD3- inducer cells: evidence that IL-7 signals regulate CD30 ligand but not OX40 ligand expression. J Immunol 2005;174:6686.
[35] Baba E, Takahashi Y, Lichtenfeld J, Tanaka R, Yoshida A, Sugamura K, Yamamoto N, Tanaka Y. Functional CD4 T cells after intercellular molecular transfer of OX40 ligand. J Immunol 2001;167:875.
[36] Ma BY, Mikolajczak SA, Danesh A, Hosiawa KA, Cameron CM, Takaori-Kondo A, Uchiyama T, Kelvin DJ, Ochi A. The expression and the regulatory role of OX40 and 4-1BB heterodimer in activated human T cells. Blood 2005;106:2002.
[37] Ito T, Wang YH, Duramad O, Hori T, Delespesse GJ, Watanabe N, Qin FX, Yao Z, Cao W, Liu YJ. TSLP-activated dendritic cells induce an inflammatory T helper type 2 cell response through OX40 ligand. J Exp Med 2005;202:1213.
[38] Mangan PR, Harrington LE, O'Quinn DB, Helms WS, Bullard DC, Elson CO, Hatton RD, Wahl SM, Schoeb TR, Weaver CT. Transforming growth factor-beta induces development of the T(H)17 lineage. Nature 2006;441:231.
[39] Wahl SM, Wen J, Moutsopoulos N. TGF-beta: a mobile purveyor of immune privilege. Immunol Rev 2006;213:213.
[40] Chen W, Jin W, Hardegen N, Lei KJ, Li L, Marinos N, McGrady G, Wahl SM. Conversion of peripheral CD4 CD25 naive T cells to CD4 CD25 regulatory T cells by TGF-beta induction of transcription factor Foxp3. J Exp Med 2003;198:1875.
[41] Li MO, Sanjabi S, Flavell RA. Transforming growth factor-beta controls development, homeostasis, and tolerance of T cells by regulatory T cell-dependent and -independent mechanisms. Immunity 2006;25:455.

Microbiol. Immunol., 51(2), 235–242, 2007

Autonomous Proliferation of HTLV CD4 T Cell Clones Derived from Human T Cell Leukemia Virus Type I (HTLV-I)-Associated Myelopathy Patients

Naoko Miyano-Kurosaki*[,1], Jun-ichi Kira[2], Jacob Samson Barnor[1], Naoyoshi Maeda[3], Naoko Misawa[4], Yuji Kawano[2], Yuetsu Tanaka[5], Naoki Yamamoto[6], and Yoshio Koyanagi[4]

[1]*Department of Life and Environmental Sciences and High Technology Research Center, Chiba Institute of Technology, Narashino, Chiba 275–0016, Japan,* [2]*Department of Neurology, Neurological Institute, Graduate School of Medical Sciences, Kyushu University, Fukuoka, Fukuoka 812–8582, Japan,* [3]*Division of Host Defense, Research Center for Prevention of Infectious Disease, Medical Institute of Bioregulation, Kyushu University, Fukuoka, Fukuoka 812–8582, Japan,* [4]*Laboratory of Viral Pathogenesis, Institute for Virus Research, Kyoto University, Kyoto, Kyoto 606–8507, Japan,* [5]*Department of Immunology, Graduate School and Faculty of Medicine, University of the Ryukyus, Okinawa 903–0215, Japan and* [6]*Department of Molecular Virology, Tokyo Medical and Dental University Graduate School of Medicine, Bunkyo-ku, 113–8510, Japan*

Received October 31, 2006; Accepted November 17, 2006

Abstract: **That HTLV-I infects CD4 T cells and enhances their cell growth has been shown as successful long-term *in vitro* proliferation in the presence of IL-2. It is known that T cells isolated from HAM patients possess strong ability for cell proliferation *in vitro* and mRNA of various cytokines are abundantly expressed in CNS tissues of HAM patients. Hence, the cytokine-induced proliferation could have an important role in pathogenesis and immune responses of HAM. In this study, we examined the relationship between cell proliferation and ability of *in vitro* cytokine production of CD4 T cell clones isolated from HAM patients. We started a culture from a single cell to isolate cell clones immediately after drawing blood from the patients using limiting dilution method, which could allow the cell to avoid *in vitro* HTLV-I infection after initiation of culture. Many cell clones were obtained and the rate of proliferation efficiency from a single cell was as high as 80%, especially in the 4 weeks' culture cells from HAM patients. These cells were classified as mainly Th0 phenotype that produce both IFN- and IL-4 after CD3-stimulation. However, the frequency of proviral DNA in these cloned cells was significantly low. Our results indicate that the ability of cell proliferation in HAM patients is not restricted in HTLV-I-infected T cells. HTLV-I-uninfected CD4 T cells, mainly Th0 cells, also have a strong ability to respond to IL-2-stimulation, showing that unusual immune activation on T cells has been observed in HAM patients.**

Key words: **HTLV-1, HAM, Clone, Self-proliferation, Limiting-dilution**

Human T cell lymphotropic virus type I (HTLV-I) is the etiological agent for adult T cell leukemia (ATL) and HTLV-I-associated myelopathy (HAM) (5, 13, 17). A single clone of HTLV-I provirus-integrated cells (leukemic cells) expands in peripheral blood of ATL patients, while multiple clones of the randomly integrated cells are frequently detected in HAM patients (22). Furthermore, a larger number of HTLV-I-infected cells are found in peripheral blood of HAM patients than that in asymptomatic carriers (21). Although HTLV-I induces T cell transformation, characterized as permanent cell growth without any stimulation, HTLV-I also more frequently induces T cell immortalization, characterized as continuous cell growth *in vitro* with cytokine-stimulation such as IL-2-stimulation. This characteristic allows the generation of T cell lines

**Address correspondence to* Dr. Naoko Miyano-Kurosaki, Department of Life and Environmental Sciences, Chiba Institute of Technology, 2–17–1 Tsudanuma, Narashino, Chiba 275–0016, Japan. Fax: 81–47–478–0414. E-mail: nkurosaki@sun.it-chiba.ac.jp

Abbreviations: ATL, adult T cell leukemia; FBS, fetal bovine serum; HAM, HTLV-I-associated myelopathy; HAM/TSP, HTLV-I-associated myelopathy/tropical spastic paraparesis; HTLV-I, human T cell lymphotropic virus type I; IgG_1, immunoglobulin G_1; IL-2, interleukin-2; IL-4, interleukin-4; MMC, mitomycin C; MS, multiple sclerosis; PBL, peripheral blood lymphocytes; TCR, T cell receptor.

through its orchestrated machinery of cytokine- and HTLV-I-induced signal transductions, suggesting that the cytokine dependency is the outcome of HTLV-I infection. Thus, it is interesting to know what mechanism is involved in the efficient cell proliferation of HTLV-I-infected and -uninfected T cells in this disease. The aim of the present study is to compare the characteristics of T cells from healthy HTLV-I-infected carriers to those from HAM patients in the proliferating nature, the presence of HTLV-I DNA and the production of immunoregulatory cytokines. Hence, for this purpose, we first generated cell clones of CD4 T cells isolated from HAM patients and healthy individuals and evaluated their ability to proliferate *in vitro*. Furthermore, we examined the cytokine production in relation to the proliferation nature of the cloned T cells in an attempt to clarify HTLV-I infection in these cells.

To generate CD4 T cells, peripheral blood lymphocytes (PBL) from the patients with HAM or other neurological diseases and healthy individuals including HTLV-I-infected persons were isolated from heparinized venous blood by Ficoll-Hypaque density gradient centrifugation and CD4 T cells were purified using CD4 magnetic beads (Dynal Biotech, Wis., U.S.A.) as recommended by the manufacturer. CD4 T cell clones were obtained in limiting dilution in 96-well round-bottomed plates at final concentrations of 1 cell per well. To prepare allogeneic feeder cells, cells from HTLV-I-negative healthy donors were treated with 50 μg/ml of mitomycin C (MMC) (Sigma-Aldrich Co., St. Louis, Mo., U.S.A.) for 30 min. After washing, these cells were added at a concentration of $5.0\ 10^3$ cells/well and cultured in RPMI 1640 containing 12% fetal bovine serum (FBS) in the presence of 100 IU/ml of human recombinant interleukin-2 (rIL-2; Shionogi Pharmaceutical, Osaka, Japan).

At the time points of 4, 6, and 8 weeks after initiation of culture, we found that the cloned CD4 T cells from some HAM patients efficiently proliferated from a single cell through an unusual growth ability (Table 1). Cell cloning efficiency was calculated based on the number of proliferated clones per total numbers of wells and expressed as a percentage. It was noteworthy that the cloning efficiencies from 7 HAM patients were more than 80% (4 weeks). Interestingly, this phenomenon was not observed in the clones isolated from patients with multiple sclerosis (MS), Sjogren syndrome, or cervical spondylosis except for 2 HTLV-I MS patients (31 and 34). Such proliferation (immortalization) was observed in 18 (69%) out of a total of 26 HAM patients. Notably, the differences were observed in the proliferation pattern of clones originating from the same HAM patients cultured over intervals of 4, 6, and 8 weeks (Table 1). No striking relation was noted with the titer of HTLV-I antibody or with or without any form of treatment among these HAM patients.

In addition, we examined T cell receptor (TCR) usage in some cloned cells using a series of FITC-conjugated mouse monoclonal antibodies (mAbs) against individual TCR-α and β molecules. After incubation with these mAbs, the cells were fixed by 0.5% paraformaldehyde and analyzed on a Becton Dickinson FACSCalibur with CellQuest software. Data of the specific TCR molecules in these clones indicated that Vα2, Vβ5(a) and Vβ8(a) were predominant TCR members induced in these HAM patients (Table 3).

Next, we examined cytokine production from these cloned T cells after stimulation with an anti-CD3 mAb. After 1 day of priming, the cytokine content of the resulting supernatants was measured by enzyme-linked immunosorbent assay (ELISA). Six days after initial stimulation, the proliferated cloned T cells were further restimulated with an anti-CD3 mAb to confirm the cytokine profile of the individual cultures. Measuring IFN-γ and IL-4 in the cell supernatants served to monitor the development of Th0, Th1 and Th2 phenotypes. Clones that produced detectable levels of both IFN-γ and IL-4 were considered to belong to Th0 subtype, clones that produced IFN-γ but no detectable (10 pg/ml) IL-4 were considered to be Th1, while clones that produced IL-4 but no detectable IFN-γ (25 pg/ml) were considered to be Th2. The cloned T cells from HAM patient #15, which exhibited significant proliferation ability in the 4- to 8-week cultures, showed that the development of the most Th subtype was Th0 (83.1% of clones), and some was Th1 (15.7%) and Th2 (1.1%), while that of patient #2 showed that many Th subtypes were also Th0 (78.5%) and Th1 (21.4%), and that of patient #4 showed that many subtypes were Th0 (89.3%) and Th1 (10.6%) (Fig. 1) (Table 2).

To determine HTLV-I infection, we extracted DNA from these cloned cells and subjected them to nested PCR to amplify the Tax region. The primers used for the first step of PCR were Tax 7307 (5'-TTC CCA GGG TTT GGA CAG A-3'; HTLV-I position 7307–7325) and Tax 7552 (5'-GAC CCT CAA GGT CCT TAC CC-3'; HTLV-I position 7552–7571), and those used for the second step of PCR were Tax 7336 (5'- CGG ATA CCC AGT CTA CGT -3'; HTLV-I position 7336–7353) and Tax 7474 (5'-CGA TGG ACG CGT TAT CGG CTC -3'; HTLV-I position 7474–7494). The final PCR mixture (25 μl) consisted of 50 mM KCl, 10 mM Tris-HCl (pH 8.3), 1.5 mM $MgCl_2$, 0.1% gelatin, 0.25 mM of each dNTP, 100 ng each of oligonucleotide primer, and 0.75 U of *Taq* polymerase (Cetus, Calf.,

Table 1. Sex, age, antibody titers and rate self-proliferation of clones from patients with HTLV-1-associated diseases and healthy donors

Patient No.	Diagnosis	Sex	Age	HTLV-Ab (titer)	Medication	Cloning efficiency (%)		
						4W	6W	8W
1	HAM	F	74	16,384	Vitamin C	3.1	12.5	40.6
2	HAM	F	58	4,096		85.9	36.4	32.8
3	HAM	F	56	512	Vitamin C	0	0	0
4	HAM	F	56	512	Vitamin C	96.8	40.1	31.2
5	HAM	F	56	512	Vitamin C	13	9.3	5.2
6	HAM	F	46	16,384	Vitamin C	92.7	90.1	91.6
7	HAM	F	46	n.d.**	Vitamin C	0	0	0
8	HAM	F	48	8,192	Vitamin C	88	58.8	58.8
9	HAM	F	63	8,192	IFN-α	88.5	76.5	46.8
10	HAM	F	63	8,192	IFN-α	1.5	1.5	1
11	HAM	F	66	8,192	IFN-α	0.5	0	0
12	HAM	F	66	8,192	IFN-α	0	0	0
13	HAM	F	39	8,192	IFN-α	44.2	29.6	29.6
14	HAM	M	46	256		93.2	45.3	10.4
15	HAM	F	60	2,560	Vitamin C	83.3	58.3	57.2
16	HAM	F	56	8,192	IFN-α, Vitamin C	0	0	0
17	HAM	F	64	8,192		75.5	53.6	41.6
18	HAM	M	71	8,192	Vitamin C	5.2	0.5	2
19	HAM	M	71	8,192	Vitamin C	2	2	2
20	HAM	F	36	32,768	Vitamin C	8.3	23.4	23.4
21	HAM	F	36	32,768	Vitamin C	2	2	2
22	HAM	F	36	32,768	Vitamin C	67.7	60.9	40.6
23	HAM	F	55	16,384		0	0	0
24	HAM	M	40	16,384	IFN-α	0.5	0.5	0.5
25	HAM	M	37	2,048	IFN-α	0	0	0
26	HAM	F	61	320	IFN-α	0	0	0
27	MS	M	40	n.d.		0	0	0
28	MS	F	20	n.d.		0	0	0
29	MS	F	50	n.d.		0	0	0
30	MS	F	46	n.d.		0	0	0
31	MS	F	73	16,384	Vitamin C	2	14.5	29.1
32	MS	F	73	16,384	Vitamin C	0	0	0
33	MS	F	36	n.d.		0	0	0
34	MS	F	53	32,768		0.5	0.5	0.5
35	MS	F	*	n.d.		0	0	0
36	MS	F	55	2,048		0	0	0
37	MS	F	55	2,048		0	0	0
38	MS	F	57	n.d.	Predonine	1	0.5	0.5
39	Sjogren	F	59	2,024		0	0	0
40	Cervical spondylosis	M	61	2,048		0	0	0
41	Cervical spondylosis	M	61	2,048		0	0	0
42	Healthy	F	29	n.d.		0	0	0
43	Healthy	M	39	n.d.		0	0	0
44	Healthy	M	31	n.d.		0	0	0

*: unknown.
n.d.**: not detected.

U.S.A.). The reaction mixture was subjected to 30 cycles of PCR amplification: denaturation for 1 min at 94 C, annealing for 1 min at 58 C (62 C in the first cycle), and polymerization for 1 min at 72 C. Then, 2 μl of the product from the first step of PCR was subjected to a second PCR step under the same conditions. The PCR product (159 bp) was analyzed by electrophoresis on 8% non-denaturing polyacrylamide gels and stained with ethidium bromide (data not shown). These extracted DNA were also subjected to β-globin-

Table 2. Cytokine production and Th subtypes detected in clones from HAM patients*

No.	Clone	IFN-γ (pg/ml)	IL-4 (pg/ml)	Th subtype	No.	Clone	IFN-γ (pg/ml)	IL-4 (pg/ml)	Th subtype	No.	Clone	IFN-γ (pg/ml)	IL-4 (pg/ml)	Th subtype
1	A1A2	14,000	176	0	59	N1D4	1,874	188	0	118	N2F10	14,408	5.12	1
2	A1A3	11,430	6,424	0	60	N1D6	1,701	59	0	119	N2G1	13,306	531	0
3	A1A4	17,080	5.12	1	61	N1D9	2,005	11	0	120	N2G4	11,100	1,378	0
4	A1A5	312	5.12	1	62	N1D11	2,084	385	0	121	N2G5	3,188	12	0
5	A1A9	27,540	1,963	0	63	N1E5	247	5.12	1	122	N2G6	14,215	79	0
6	A1B7	25,700	630	0	64	N1E9	1,744	185	0	123	N2G7	13,559	860	0
7	A1B8	30,220	592	0	65	N1E10	1,754	84	0	124	N2G10	10,564	5.12	1
8	A1B9	28,300	3,344	0	66	N1E11	1,460	5.12	1	125	N2G11	2,658	502	0
9	A1B12	13,412	6,804	0	67	N1F9	2,120	5.12	1	126	N2H5	13,396	1,419	0
10	A1C4	6,574	5.12	1	68	N1G2	1,319	5.12	1	127	N2H6	11,805	743	0
11	A1C6	1,974	84	0	69	N1G4	543	84	0	128	N2H9	14,306	3,248	0
12	A1D5	9,732	2,554	0	70	N1G8	1,414	5.12	1	129	N2H11	13,993	5.12	1
13	A1D8	25,880	26	0	71	N1G9	2,113	186	0	130	F3A2	1,620	191	0
14	A1E7	28,740	5.12	1	72	N1G10	707	5.12	1	131	F3A5	2,033	54	0
15	A1E9	18,446	3,906	0	73	N1H1	1,726	68	0	132	F3A7	2,036	12	0
16	A1F5	28,820	4,408	0	74	N1H2	1,559	5.12	1	133	F3A9	787	110	0
17	A1F8	29,780	247	0	75	N1H4	101	15	0	134	F3B8	1,369	5.12	1
18	A1F12	27,000	537	0	76	N1H5	153	55	0	135	F3B9	1,926	316	0
19	A1G10	7,366	518	0	77	N1H8	2,088	76	0	136	F3B11	577	203	0
20	A1H9	13,028	189	0	78	N1H9	453	18	0	137	F3B12	2,057	5.12	1
21	A1H10	27,020	3,124	0	79	N1H10	2,127	491	0	138	F3C1	1,911	208	0
22	A2A5	555	5.12	1	80	N1H11	1,892	348	0	139	F3C5	1,142	410	0
23	A2A7	2,204	5,440	0	81	N2A3	3,161	740	0	140	F3C8	1,926	184	0
24	A2A12	20,600	5.12	1	82	N2A7	12.8	2,864	2	141	F3C11	731	194	0
25	A2B2	24,960	5,750	0	83	N2A10	22,000	4,792	0	142	F3C12	1,734	5.12	1
26	A2B7	26,120	23	0	84	N2A11	5,088	5.12	1	143	F3D2	1,066	459	0
27	A2C1	2,204	1,465	0	85	N2B1	25,529	4,819	0	144	F3D5	145	5.12	1
28	A2C4	28,420	614	0	86	N2B2	13,775	4,450	0	145	F3E1	1,828	276	0
29	A2C5	29,600	1,976	0	87	N2B3	17,874	5.12	1	146	F3E3	12,714	381	0
30	A2C6	21,920	422	0	88	N2B4	27,633	6,252	0	147	F3E4	7,907	25	0
31	A2C10	28,700	825	0	89	N2B5	18,729	4,535	0	148	F3E6	3,924	136	0
32	A2C12	25,580	1,260	0	90	N2B6	8,957	248	0	149	F3E7	789	2,905	0
33	A2E6	30,180	5.12	1	91	N2B8	18,770	720	0	150	F3E8	10,150	1,609	0
34	A2E7	27,900	582	0	92	N2B11	21,254	425	0	151	F3E11	10,150	5.12	1
35	A2E8	1,488	5.12	1	93	N2C2	31,216	3,740	0	152	F3E12	13,347	1,084	0
36	A2F5	7,904	3,942	0	94	N2C3	29,194	1,347	0	153	F3F3	1,349	5.12	1
37	A2F9	8,428	5.12	1	95	N2C4	3,270	7,565	0	154	F3F4	14,361	928	0
38	A2G6	427	704	0	96	N2C5	29,750	693	0	155	F3F7	1,619	1,949	0
39	A2H7	1,706	80	0	97	N2C8	215	5.12	1	156	F3F10	7,932	213	0
40	A2H11	7,878	5.12	1	98	N2C9	1,071	5.12	1	157	F3G6	14,164	3,762	0
41	N1A2	6,554	617	0	99	N2D1	23,710	175	0	158	F3G9	4,029	1,490	0
42	N1A5	7,016	5.12	1	100	N2D3	6,934	14	0	159	F3H9	7,231	4,251	0
43	N1A8	12.8	1,097	2	101	N2D5	11,630	3,371	0	160	F4A3	3,568	1,818	0
44	N1A12	21,716	1,965	0	102	N2D7	10,286	7,396	0	161	F4A5	14,201	469	0
45	N1B3	30,769	2,415	0	103	N2D8	27,782	1,055	0	162	F4B11	12,726	5.12	1
46	N1B8	20,603	1,189	0	104	N2D9	11,329	3,736	0	163	F4C3	14,041	1,291	0
47	N1B9	29,982	209	0	105	N2E1	1,025	830	0	164	F4C4	13,851	1,093	0
48	N1B10	25,964	148	0	106	N2E3	4,851	1,635	0	165	F4C7	13,617	496	0
49	N1B11	31,095	1,162	0	107	N2E4	211	5.12	1	166	F4C8	12,240	906	0
50	N1C1	9,283	655	0	108	N2E5	10,479	424	0	167	F4C11	7,735	1,109	0
51	N1C2	5,387	490	0	109	N2E7	12,661	2,373	0	168	F4E5	7,618	3,932	0
52	N1C4	5,346	3,555	0	110	N2E8	10,437	5.12	1	169	F4E6	193	728	0
53	N1C5	19,598	352	0	111	N2E9	7,834	290	0	170	F4E11	10,009	4,138	0
54	N1C6	12,567	367	0	112	N2E10	13,390	2,834	0	171	F4F1	13,279	779	0
55	N1C8	16,856	1,024	0	113	N2F1	416	3,490	0	172	F4G2	12,923	2,096	0
56	N1C10	26,344	6,839	0	114	N2F3	13,324	303	0	173	F4G3	14,281	5.12	1
57	N1D1	9,527	1,374	0	115	N2F4	2,465	202	0	174	F4G12	2,050	1,172	0
58	N1D3	2,171	35	0	116	N2F5	4,339	416	0	175	F4H2	12,197	549	0
					117	N2F6	12,914	1,344	0	176	F4H12	248	617	0

*Cloned cells were stimulated with immobilized CD3 mAb and 24 hr later, the cytokine concentration in the culture supernatant was measured.

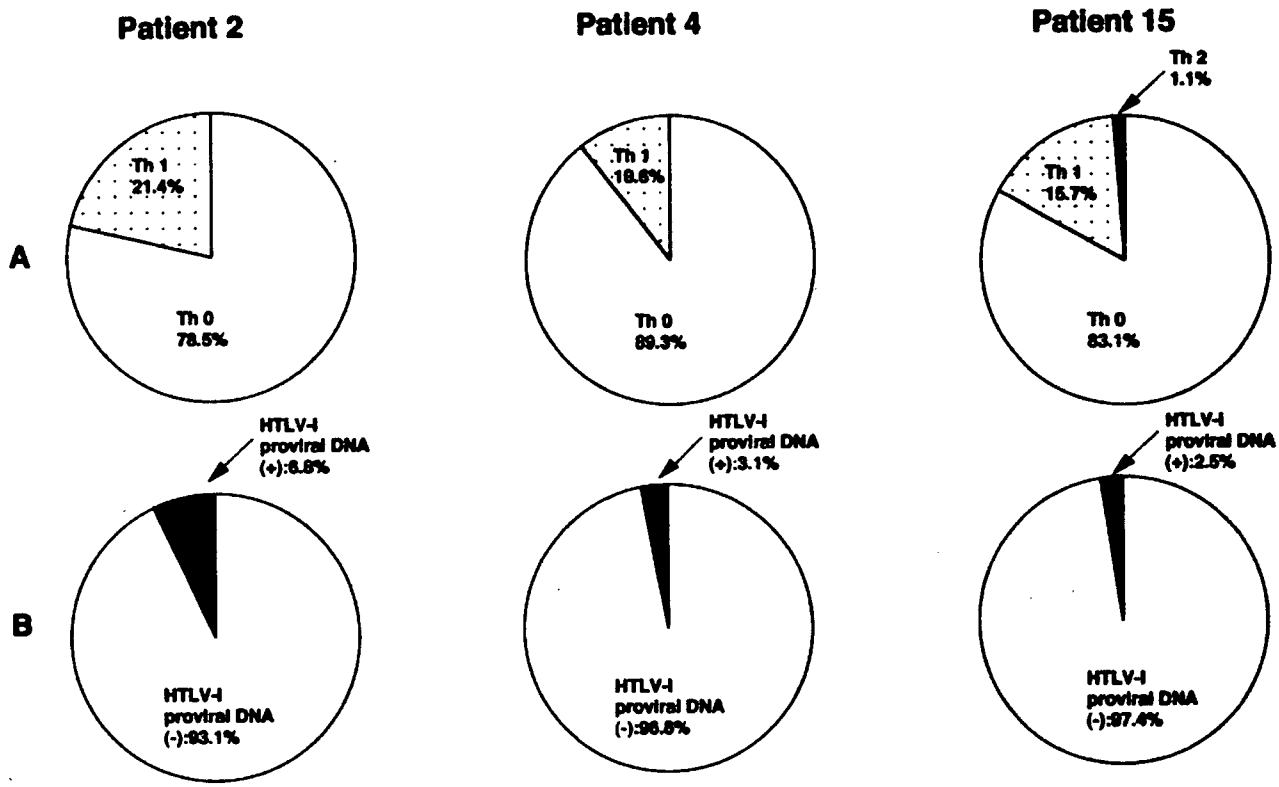

Fig. 1. Pie chart representation of Th subtypes and proviral DNA integration in clones. A. Cloned CD4+ T cells from healthy carriers and HAM patients were stimulated with OKT3 antibody, and then levels of IFN-γ and IL-4 were measured by ELISA to determine the profile of Th subtypes. B. PCR detection of HTLV-I proviral DNA integration in clones from the same subjects.

specific PCR as an internal control described previously. Results from the PCR indicated that only 10 cloned samples (4.35%) out of a total of 230 samples tested were positive for HTLV-1 proviral DNA. Out of the cloned cells derived from patient #15, only 2.5% of the clones possessed the proviral DNA, while 97.4% showed HTLV-I-negative. Similarly, in patients #2 and #4, 6.8% and 3.1% clones, respectively, possessed the proviral DNA, while others, 93.1% and 96.8%, respectively, were negative. Furthermore, from 3 selected clones, 10–20% exhibited a Th1 response while 80–90% showed a Th0 response. Only one of the three patients had clones with a Th2 response (Fig. 1). These results affirmed the fact that HTLV-I randomly integrated and also that many CD4+ T cells escaped from the infection in HAM patients (23).

To ascertain whether proliferating cloned T cells are susceptible to apoptosis, an anti-Fas antibody was added to the culture and induction of cell death was examined 24 hr later. Five out of the 15 tested clones, which comprised both clones with or without HTLV-I proviral DNA, were apoptosis-sensitive (Table 3). Therefore, these results implied that both cloned cells are not Fas-reactive transformed cells.

In this study, we described the successful generation of HTLV-I as well as HTLV cell clones from HAM patients. These CD4+ T cell clones originating from some of the fresh peripheral blood samples of HAM patients showed unusual proliferation characteristics from a single cell. This phenomenon was observed in 18 out of 26 HAM patients. We also noted differences in the actively proliferating periods among the clones derived from the same patient, and culture over different time frames. There was no direct relationship drawn between the titer of HTLV-I antibody and the extent of the cell proliferation. Importantly, there was also no direct correlation between HTLV-1 infection and the ability of abnormal proliferation observed in cell clones. The rate of HTLV-I infection was very rare (2.5 to 6.8%). These findings are in conformity with other results (23). The predominantly represented TCRαβ were Vα2, Vβ5(a), and Vβ8(a). Despite the relatively very low rate of HTLV-I-induced immortalization in the absence of IL-2, long-term culture was achieved in propagated clones detected for IL-4. IL-4-dependent transformants clearly depend on this cytokine for

Table 3. Characteristics of clones derived from HAM patients

Clone	Th subtype	Viral DNA	TCR usage	Apoptosis sensitivity
N1G8	Th 1		Vβ5(a)	
N2E4	Th 1		Vβ8(a)	n.t.
N2A7	Th 2		Vα2	n.t.
A2B2	Th 0		Vβ5(a)	n.t.
F4C3	Th 0		n.d.	n.t.
N1B10	Th 0		Vα2	n.t.
N1C10	Th 0		Vβ8(a)	n.t.
N1C4	Th 0		Vβ5(a)	
N1D9	Th 0		n.d.	n.t.
N1E9	Th 0		Vα2	n.t.
N2B4	Th 0		Vβ8(a), (b)	n.t.
N2D7	Th 0		Vα2,Vβ5(a)	
N2E10	Th 0		Vα2	
N2G11	Th 0		n.d.	n.t.
N2H6	Th 0		Vα5(a), Vβ8(a)	

n.d.: not determined.
n.t.: not tested.

cytokine-mediated mitogenesis, as evidenced by the failure of cell growth when the cytokine is excluded from the growth medium. One of the most important immunological observations of HTLV-I infection is the demonstration that lymphocytes spontaneously proliferate *in vitro* in the absence of stimulus (15).

The pathogenesis of HAM/TSP is not yet understood. Although initially considered a rare and late complication of infection, the disease has been identified in children, and a rapidly progressive disease has been observed in some patients (8). Increased proviral load, pro-inflammatory cytokines and the expansion of HTLV-I tax-specific CD8 cytotoxic T lymphocytes, both in cerebrospinal fluid and in peripheral blood, have been associated with central nervous system involvement in patients with HAM/TSP (1, 6, 9, 10, 12). A recent report (19) described a cohort of HTLV-I asymptomatic carriers and documented an increased frequency of abnormalities, including a case of HAM. Evaluation of immunological responses in patients with HAM and asymptomatic carriers is important for the understanding of the pathogenesis of the disease, and to identify early immunological markers associated with progression of the disease. The documentation shows that some HTLV-I carriers have an immunological alteration similar to that observed in HAM, suggesting that potential markers of disease progression may be available in HTLV-I infection. Many studies have demonstrated that IFN-γ and TNF-α, if produced in large quantities, contribute to tissue damage in the central nervous system (2, 20) and are likely involved in the pathogenesis of several infectious and non-infectious diseases. The flow cytometric determination of cytokine-producing lymphocytes extends the observations made in supernatants of lymphocyte cultures showing a significant increase in the frequency of IFN-γ and TNF-α producing cells in patients with HAM/TSP. The increased frequency of TNF-α producing cells was accounted for by both CD4 and CD8 T cells, and the increase in IFN-γ producing lymphocytes mainly by CD8 T cells. In HTLV-I carriers, CD4 T cells are the main source of IFN-γ (3, 14, 16); therefore, these data may indicate that during the progression from asymptomatic infection to myelopathy there is a switch from CD4 to CD8 in relation to the main cells producing IFN-γ. These findings support studies suggesting that CD8 T cells may play an important role in the pathogenesis of HAM (18). Muniz et al. showed the validity of the neurological scales to classify the degree of neurological disability in HTLV-I carriers and suggested a progressive behavior of HAM/TSP and IFN-γ in PBMC supernatants were markers of HAM/TSP. There was no correlation between neurological disability and cytokine levels; on the other hand, there were elevated levels of helper T cell 1 (Th1) cytokines in PBMC with different degrees of neurological disability, suggesting a state of constant inflammatory activity (steady-state). However, there was a trend toward an inverse correlation of IFN-γ, TNF-α, IL-10 and IL-5 levels in unstimulated PBMC with time of illness duration, showing a slight decrease of inflammatory response over time (11). Kaneyasu et al. suggested that IFN-γ augmented the anti-viral effect by enhancing innate immunity and shifting the immune response to Th1 (7). Fujimoto et al. demonstrated that IL-12 was one of the critical factors for Th1 development. However, they herein found that anti-IL-12 did

not completely prevent Th1 development and IL-12 did not induce Th1 development without TCR signaling (4). Therefore, it remains possible that the quality of TCR signaling also plays an important role in regulation of Th development.

Although many of the clones lacked HTLV-I proviral DNA, they all exhibited a Th0 response. Hence, the lack of proviral DNA in these clones suggests that there could be a direct relationship between cloning efficiency and the type of cytokine response induced. Our findings could not fully establish the mechanism by which T lymphocyte clones that lack HTLV-1 proviral DNA nevertheless exhibit unusual proliferation. Thus, further studies will be required to unveil all the mechanistic processes underlining the observed phenomenon.

This work was supported by grants from the Ministry of Health, Labour and Welfare and the Ministry of Education, Culture, Sports, Science and Technology, Japan.

References

1) Azimi, N., Mariner, J., Jacobson, S., and Waldmann, T.A. 2000. How does interleukin 15 contribute to the pathogenesis of HTLV type 1-associated myelopathy/tropical spastic paraparesis? AIDS Res. Hum. Retroviruses **16**: 1717–1722.
2) Biddison, W.E., Kubota, R., Kawanishi, T., Taub, D.D., Cruikshank, W.W., Center, D.M., Connor, E.W., Utz, U., and Jacobson, S. 1997. Human T cell leukemia virus type I (HTLV-I)-specific CD8 CTL clones from patients with HTLV-I-associated neurologic disease secrete proinflammatory cytokines, chemokines, and matrix metalloproteinase. J. Immunol. **159**: 2018–2025.
3) Carvalho, E.M., Bacellar, O., Porto, A.F., Braga, S., Galvao-Castro, B., and Neva, F. 2001. Cytokine profile and immunomodulation in asymptomatic human T-lymphotropic virus type 1-infected blood donors. J. Acquir. Immune Defic. Syndr. **27**: 1–6.
4) Fujimoto, N., Ishida, H., Nakamura, I., Ogasawara, K., and Itoh, Y. 2003. Quantities of interleukin-12p40 in mature CD8 alpha negative dendritic cells correlate with strength of TCR signal and determine Th cell development. Microbiol. Immunol. **47**:1017–1024.
5) Gessain, A., Barin, F., and Vernant, J.C. 1985. Antibodies to human T-lymphotropic virus type I in patients with tropical spastic paraparesis. Lancet **2**: 407–410.
6) Hanon, E., Hall, S., Taylor, G.P., Saito, M., Davis, R., Tanaka, Y., Usuku, K., Osame, M., Weber, J.N., and Bangham, C.R. 2000. Abundant tax protein expression in CD4 T cells infected with human T-cell lymphotropic virus type I (HTLV-I) is prevented by cytotoxic T lymphocytes. Blood **95**: 1386–1392.
7) Kaneyasu, K., Kita, M., Ohkura, S., Yamamoto, T., Ibuki, K., Enose, Y., Sato, A., Kodama, M., Miura, T., and Hayami, M. 2005. Protective efficacy of nonpathogenic nef-deleted SHIV vaccination combined with recombinant IFN-gamma administration against a pathogenic SHIV challenge in rhesus monkeys. Microbiol Immunol. **49** 1083–1094.
8) Kramer, A., Maloney, E.M., Morgan, O.S., Rodgers-Johnson, P., Manns, A., Murphy, E.L., Larsen, S., Cranston, B., Murphy, J., Benichou, J., et al. 1995. Risk factors and cofactors for human T-cell lymphotropic virus type I (HTLV-I)-associated myelopathy/tropical spastic paraparesis (HAM/TSP) in Jamaica. Am. J. Epidemiol. **142**: 1212–1220.
9) Kubota, R., Kawanishi, T., Matsubara, H., Manns, A., and Jacobson, S. 2000. HTLV-I specific IFN-gamma CD8 lymphocytes correlate with the proviral load in peripheral blood of infected individuals. J. Neuroimmunol. **102**: 208–215.
10) Miller, G., and Lipman, M. 1973. Release of infectious Epstein-Barr virus by transformed marmoset leukocytes. Proc. Natl. Acad. Sci. U.S.A. **70**: 190–194.
11) Muniz, A.L., Rodrigues, W., Jr., Santos, S.B., de Jesus, A.R., Porto, A.F., Castro, N., Oliveira-Filho, J., Almeida, J.P., Moreno-Carvalho, O., and Carvalho, E.M. 2006. Association of cytokines, neurological disability, and disease duration in HAM/TSP patients. Arq. Neuropsiquiatr. **64**: 217–221.
12) Nagai, M., and Jacobson, S. 2001. Immunopathogenesis of human T cell lymphotropic virus type I-associated myelopathy. Curr. Opin. Neurol. **14**: 381–386.
13) Nagai, M., Usuku, K., Matsumoto, W., Kodama, D., Takenouchi, N., Moritoyo, T., Hashiguchi, S., Ichinose, M., Bangham, C.R., Izumo, S., and Osame, M. 1998. Analysis of HTLV-I proviral load in 202 HAM/TSP patients and 243 asymptomatic HTLV-I carriers: high proviral load strongly predisposes to HAM/TSP. J. Neurovirol. **4**: 586–593.
14) Osame, M., Usuku, K., Izumo, S., Ijichi, N., Amitani, H., Igata, A., Matsumoto, M., and Tara, M. 1986. HTLV-I associated myelopathy, a new clinical entity. Lancet **1**: 1031–1032.
15) Popovic, M., Lange-Wantzin, G., Sarin, P.S., Mann, D., and Gallo, R.C. 1983. Transformation of human umbilical cord blood T cells by human T-cell leukemia/lymphoma virus. Proc. Natl. Acad. Sci. U.S.A. **80**: 5402–5406.
16) Prince, H., Kleinman, S., Doyle, M., Lee, H., and Swanson, P. 1990. Spontaneous lymphocyte proliferation *in vitro* characterizes both HTLV-I and HTLV-II infection. J. Acquir. Immune Defic. Syndr. **3**: 1199–1200.
17) Richardson, J.H., Edwards, A.J., Cruickshank, J.K., Rudge, P., and Dalgleish, A.G. 1990. *In vivo* cellular tropism of human T-cell leukemia virus type 1. J. Virol. **64**: 5682–5687.
18) Roman, G.C., and Osame, M. 1988. Identity of HTLV-I-associated tropical spastic paraparesis and HTLV-I-associated myelopathy. Lancet **1**: 651.
19) Sakai, J.A., Nagai, M., Brennan, M.B., Mora, C.A., and Jacobson, S. 2001. *In vitro* spontaneous lymphoproliferation in patients with human T-cell lymphotropic virus type I-associated neurologic disease: predominant expansion of CD8 T cells. Blood **98**: 1506–1511.
20) Taylor, G.P., Tosswill, J.H., Matutes, E., Daenke, S., Hall, S., Bain, B.J., Davis, R., Thomas, D., Rossor, M., Bangham, C.R., and Weber J.N. 1999. Prospective study of

HTLV-I infection in an initially asymptomatic cohort. J. Acquir. Immune Defic. Syndr. **22**: 92–100.
21) Umehara, F., Izumo, S., Ronquillo, A.T., Matsumuro, K., Sato, E., and Osame, M. 1994. Cytokine expression in the spinal cord lesions in HTLV-I-associated myelopathy. J. Neuropathol. Exp. Neurol. **53**: 72–77.
22) Yoshida, M., Osame, M., Kawai, H., Toita, M., Kuwasaki, N., Nishida, Y., Hiraki, Y., Takahashi, K., Nomura, K., Sonoda, S., Eiraku, N., Ijichi, S., and Usuku, K. 1989. Increased replication of HTLV-I in HTLV-I-associated myelopathy. Ann. Neurol. **26**: 331–335.
23) Yoshida, M., Osame, M., Usuku, K., Matsumoto, M., and Igata, A. 1987. Viruses detected in HTLV-I-associated myelopathy and adult T-cell leukaemia are identical on DNA blotting. Lancet **1**: 1085–1086.

AIDS RESEARCH AND HUMAN RETROVIRUSES
Volume 23, Number 3, 2007, pp. 391–397

DOI: 10.1089/aid.2006.0124

Vpr in Plasma of HIV Type 1-Positive Patients Is Correlated with the HIV Type 1 RNA Titers

SHIGEKI HOSHINO,[1,2] BINLIAN SUN,[1] MITSURU KONISHI,[3] MARI SHIMURA,[1] TATSUYA SEGAWA,[4] YOSHIAKI HAGIWARA,[4] YOSHIO KOYANAGI,[5] AIKICHI IWAMOTO,[6] JUN-ICHI MIMAYA,[7] HIROSHI TERUNUMA,[8] SHIGEYUKI KANO,[1,2] and YUKIHITO ISHIZAKA[1]

ABSTRACT

Vpr, an accessory gene product of HIV-1, has been reported in the plasma of HIV-1-positive patients, and exogenous Vpr induces the reactivation of viral production from latently infected cells and the apoptosis of T cells *in vitro*. These observations imply that Vpr is important in AIDS development, but the clinical relevance of the findings cannot be evaluated fully because the actual plasma Vpr concentration in HIV-1-positive patients is unknown. Here we generated two monoclonal antibodies against different portions of Vpr and successfully identified Vpr as a 14-kDa protein in HIV-1-positive patients. Semiquantitative analysis using a recombinant Vpr revealed that the concentration of Vpr in patient plasma was ~0.7 nM (10 ng/ml). Cross-sectional analysis of 52 HIV-1-positive patients revealed that the presence of Vpr detected in 20 patients was positively correlated with HIV-1 RNA copy number ($p < 0.03$), but not with the number of CD4$^+$ T cells. This is the first report demonstrating the actual amount of Vpr in HIV-1-positive patients, and the possible linkage of Vpr and viral titers indicates that it is important to continue to carry out the sequential analysis of Vpr, especially in clinical courses of HIV-1-positive patients. The threshold of viral titers, where Vpr appears in the patients' plasma, if present, contributes to better understanding the role of Vpr in AIDS pathogenesis.

THE ADOPTION OF ANTIRETROVIRAL THERAPY (ART) has improved the prognosis of HIV-1-positive patients.[1] However, the complete elimination of the virus from patients receiving ART is estimated to take more than 60 years.[2] One factor that may be responsible for this problem is that HIV-1 infects macrophages, latent viral reservoirs[3] from which recurrent viral production is induced by various factors.[4] *Vpr*, an accessory gene of HIV-1, encodes a virion-associated 14-kDa protein that may be critical for the primary infection of macrophages.[5–7] Vpr also induces the reactivation of viral reproduction from latently infected cells. The presence of Vpr in the sera of HIV-1-positive patients, along with the induction of viral reproduction by exogenous Vpr,[8,9] implies that Vpr is actively involved in AIDS development. However, it is necessary to determine the concentration of Vpr in patient plasma samples to correctly evaluate the clinical significance of data obtained from *in vitro* experiments. In the current study, we successfully detected Vpr in patients' samples.

The protocol of this study was approved by the ethics committees of the International Medical Centre of Japan, Nara Medical University, Shizuoka Children's Hospital, and five other hospitals in collaboration with Shizuoka Children's Hospital. Blood plasma samples and peripheral blood were obtained from patients who had given informed consent after the experiment was explained to them. Clinical data on 14 outpatients at Nara Medical University, who were enrolled in the initial study, are

[1]Research Institute, International Medical Center of Japan, Shinjuku-ku, Tokyo 162-8655, Japan.
[2]Graduate School of Comprehensive Human Sciences, University of Tsukuba, Tsukuba 305-8577, Japan.
[3]Center for Infectious Diseases, Nara Medical University, Kashihara, Nara 634-8522, Japan.
[4]Immuno-Biological Laboratories, Co., Fujioka, Gunma 375-0005, Japan.
[5]Laboratory of Viral Pathogenesis, Institute for Virus Research, Kyoto University, Sakyou-ku, Kyoto 606-8507, Japan.
[6]Department of Infectious Diseases, The Institute of Medical Science, The University of Tokyo, Minato-ku 108-8639, Tokyo, Japan.
[7]Department of Hematology and Oncology, Children's Hospital of Shizuoka Prefecture, Aoi-ku, Shizuoka 420-8660, Japan.
[8]Biotherapy Institute of Japan, Koutou-ku, Tokyo, 135-0051, Japan.

summarized in Table 1. For the second study, samples from an additional 38 patients were analyzed. The median numbers of HIV-1 RNA copies (32,289.3 copies/ml), $CD4^+$ T cells (449.4 copies/ml), and total white blood cells (5049.0 cells/ml) were determined in all 52 patients. Control healthy plasma samples were obtained from Teragenix Corporation (Kokusai Bio, Tokyo). A recombinant Vpr protein (rVpr) was first prepared as a fusion protein with glutathione *S*-transferase (GST) expressed by pGEX6-P-1, and purified according to the manufacturer's protocol (GE Healthcare Bio-Sciences, Piscataway, NJ). The purified rVpr appeared as a single band on Coomassie brilliant blue staining (supplementary information 1a: SI-1a). Two mouse monoclonal antibodies, 8D1 (IgG2a) and C217 (IgG2b), were generated by immunization with a full-length Vpr peptide, chemically synthesized based on the prototype NL4-3[10] (Osaka Peptide Institute, Osaka), and a synthetic 18-mer amino acid peptide encompassing its carboxy (C)-terminal region (Wako Pure Chemical Industries, Tokyo, Japan), respectively. An enzyme-linked immunosorbent assay (ELISA) was based on 8D1, as the primary antibody, and a purified rabbit IgG antibody, raised against the peptide of the C-terminal 18 amino acids of Vpr (IBL, Fujioka, Japan), as the second antibody. Although the Vpr-ELISA could clearly detect purified rVpr (SI-1b), we found that the system occasionally detected one or more cross-reacting peptide in healthy persons (data not shown). Therefore, we decided to carry out a semiquantitative analysis using immunoprecipitation-Western blotting (IP-WB) analysis, with rVpr quantified by ELISA as the standard. For the IP-WB analysis, 0.5 mg of C217 was bound to Protein G Sepharose (GE Healthcare Bio-Sciences). Each 200 μl of plasma was first treated with DNase I and RNase A for 5 min, and then incubated with 10 μl of C217-coupled beads for 2 h at 4°C. After being washed in buffer with 0.05% Tween-20, the immunoprecipitate was subjected to Western blot analysis. For standard samples, different amounts of purified rVpr were added to 200 μl of control plasma. No detergents were added when the samples were incubated with the primary antibody, so that the IP-WB would detect only soluble Vpr, and not Vpr in viral particles.[10] The detection limit of the system was about 1 ng/ml (0.07 nM) (SI-2a).

Representative results from the IP-WB analysis of 14 plasma samples are shown in Fig. 1a. A definite signal of the 14-kDa protein was observed in patients N-09, 11, and 13 (Fig. 1a). By contrast, no peptides around 14 kDa were detected in more than 60 specimens from healthy volunteers (Fig. 1b). Because the IP-WB could selectively detect the 14-kDa peptide in the culture supernatant of cells containing an expression plasmid encoding *vpr* (SI-2b), we concluded that the 14-kDa peptide detected by the IP–WB was Vper. A comparison of the signal intensities of the detected bands and standard rVpr (Fig. 1a; 5, 2.5, and 1.25 μg/ml signals, and N-11) indicated that the serum Vpr concentration was about 0.7 nM.

During the analysis, we did not detect the Vpr signal in one patient (N-10; Table 1) who had 11,000 copies/ml of HIV-1 RNA (Fig. 1a, lower panel). To evaluate whether our system failed to detect Vpr mutants differing from the prototype NL4-3 (GenBank accession number M19921), we amplified DNA fragments from peripheral blood mononuclear cells covering the entire *vpr* gene. Then we determined its nucleotide sequence (Fig. 2a, and primers in SI-3). The deduced amino acid sequences are also shown in Fig. 2b. Interestingly, the *vpr* gene from patient N-10 had a four-nucleotide (TTAA) insertion at

TABLE 1. CLINICAL DATA OF PATIENTS SUBJECTED TO ANALYSIS AND RESULTS OF THE IP-WB

						Clinical data				
						White blood cells (/mm³)				
Case number	*Sex*	*Age*	*Causes of infection*	*Conditions*	*Treatment status*[a]	*Total number*	*Lymphocytes*	*CD4⁺ T cells*	*HIV-1 RNA (copies/ml)*	*Vpr*[b]
N-01	M	39	HO[c]	AIDS[d]	2	8400	2612	771	<50	−
02	M	41	HO	AIDS	2	6800	2584	346	<50	−
03	M	59	HE[c]	AIDS	2	4700	2444	381	260	−
04	F	32	HE	AC[d]	3	6300	1890	302	4,400	−
05	M	38	HO	AIDS	2	8600	2417	585	<50	−
06	M	35	HO	AC	1	4900	1274	116	220,000	+++
07	M	45	BL[c]	AIDS	2	2600	546	38	73,000	++
08	M	58	HE	AIDS	2	6800	1632	366	<50	−
09	M	29	BL	AC	1	3000	1056	266	17,000	+
10	M	23	HO	AC	1	5200	1300	230	11,000	−
11	F	37	HE	AC	1	4600	1150	222	500,000	+++
12	F	40	HE	AC	1	6600	1584	598	98	−
13	M	42	BL	AIDS	2	3100	1054	110	70,000	++
14	M	23	HO	AC	1	5800	2656	553	71,000	++

[a]Group 1, no therapy; group 2, under medication; group 3, posttherapy.
[b]Based on results of the IP-WB, patients are divided into four groups; Vpr-negative (−) and Vpr-positive with less than 1 ng/ml (+), with 1–5 ng/ml (++), and with more than 5 ng/ml (+++).
[c]HO, homosexual; HE, heterosexual; BL, blood products.
[d]AIDS, acquired immunodeficiency syndrome; AC, asymptomatic carrier.

nucleotide 81, designated "clone 10," which generates a frameshift mutation within the inserted sequence (shown by the box in Fig. 2a). However, because this patient had no deletion in the 3′ region of the *vpr* gene, it was possible to clone the gene. Repeated sequence analyses of several clones of the amplified *vpr* DNA indicated that clone 10 was the major *vpr* in this patient (Table 2). The negative results of the IP-WB analysis for patient N-10 were therefore due to truncation of the C-terminal region.

Additional sequence analysis revealed that "clone N (Nara)," which differs by four amino acids from the prototype NL4-3 (Fig. 2b), was frequently observed in the analyzed patients (patients N-04, 05, 08, 09, 11, and 12). Interestingly, although patient N-09 had clone N as a major variant—all seven clones sequenced from the PCR products were identified as clone N (see Table 2)—the IP-WB analysis (Fig. 1a, lower panel) detected a positive Vpr signal in patient N-09. This suggests that C217 antibody, which was used as the first antibody in immunoprecipitation, reacts with the protein encoded by clone N, even though its C-terminal region differs from the prototype NL4-3 clone by two amino acids (Fig. 2b).

Next, we examined the possible correlation of Vpr and clinical manifestations. An analysis of 14 patients suggested a positive link between Vpr and viral titers (data not shown). To examine this possibility, we analyzed an additional 38 stocked samples using IP-WB. We detected Vpr in 14 samples. A representative result of the second analysis is shown in Fig. 1c. Positive Vpr signals were detected in patients T-166, 167, and 175. Then we examined the relationship between Vpr and RNA copy number in total 52 samples. As shown in Fig. 3a, we found a positive correlation between the detection of Vpr and RNA copy number ($p < 0.03$). In contrast, we did not detect a positive relationship between Vpr and the numbers of $CD4^+$ T cells or total white blood cells. The distribution of Vpr-positive patients based on the concentration of Vpr implied that the high amount of Vpr is observed in patients with high HIV-1 RNA copy numbers (Fig. 3b).

In the current work, we successfully identified Vpr in 20 samples from 52 HIV-1-positive patients. A comparison of the signals obtained with standard rVpr revealed that the Vpr concentration was ~0.7 nM. Levy *et al.*[9] suggested that Vpr is present in patient plasma, with rVpr activating viral reproduction when added to the culture medium of latently infected cells. In addition, Muthumani *et al.* proposed that exogenous rVpr has various activities, such as inducing T cell apoptosis,[11] inhibiting macrophage function,[12] and suppressing NF-κB signaling.[13] However, these experiments did not consider the actual amount of Vpr present in the plasma samples. Our result is the first demonstration of Vpr in HIV-1-positive patients, and provides a rationale for the dose of rVpr suitable for *in vitro* experiments.

We observed a positive correlation between the detection of Vpr and HIV-1 RNA copy number ($p < 0.03$) (Fig. 3a). It has been reported that the exogenous Vpr induces viral production from latently infected cells, implying that Vpr is involved in viral reproduction *in vivo*. An important question still to be answered is how the Vpr titer changes in the context of viral replication during the clinical course of the disease. It is important to clarify whether Vpr functions as an initial trigger of viral expansion *in vivo*.

We did not detect a link between Vpr and the numbers of $CD4^+$ T cells. Recently, it was determined that WT-Vpr and its variant R77Q act differently in modifying the clinical features of HIV-1-positive patients. Based on several reports, it has been proposed that R77Q is a candidate marker for long-term nonprogression (LTNP),[14–16] although this is still controversial.[17,18] In this study, we observed that the main Vpr variants of patients N-04, 09, and 10 were R77Q or C-terminally truncated. However, we did not recognize these patients as candidates for LTNP (clinical observation by M. Konishi). The involvement of WT-Vpr and R77Q in patients is rationalized by *in vitro* experiments showing that rVpr induces the apoptosis of $CD4^+$ T cells.[11,12,14,15] whereas R77Q has less potent apoptosis activity than WT-Vpr.[15] It is important to note that the *in vitro* studies of the differential activities of exogenous WT-Vpr and R77Q used tremendous amounts of the proteins, and a difference in activity was observed only when 1.5–2.0 μM of the peptides was used.[15] As shown here, the concentration of Vpr in patient plasma was a maximum of 1.0 nM, and it is crucial to compare the functional difference of these molecules at a concentration comparable to that observed *in vivo*. Careful studies are required to address this matter.

SUPPLEMENTARY INFORMATION

SI-1. Purification of rVpr and measurement using ELISA. (**a**) Expression and purification profiles of rVpr. Vpr was expressed as a fusion protein with GST and purified in a glutathione column. Lane 1, marker; lane 2, initial lysate; lane 3, flow-through sample eluted from the glutathione column; lane 4, eluate from rVpr after treatment with precision protease; and lane 5, eluate from an affinity column containing a monoclonal antibody against Vpr (8D1). The arrowhead and arrow indicate the position of GST-Vpr and purified rVpr, respectively. Proteins were stained with Coomassie brilliant blue solution. (**b**) ELISA verion-1 for measuring rVpr. Synthesized full-length Vpr was used to make a standard curve. To the Vpr-ELISA were added 10 ng/ml each of GAPDH, HIV-1 integrase, and SARS-CoV Spike protein, which were expressed as a (His)-tagged protein, and purified using Ni-beads. Note that none of the samples gave cross-signals with Vpr. The amount of rVpr was assessed using the absorbance at OD450 nm, as shown with the dotted line.

SI-2. Detection of Vpr by the IP-WB. (**a**) Sensitivity of the system. The IP-WB analysis was conducted using C217 for IP and 8D1 for WB. To determine the sensitivity of the system, 10, 5, 2.5, and 1.25 ng of purified rVpr were added to 200 μl of plasma from a healthy human just before the IP-WB analysis. The signals obtained using IP-WB (upper panel) and the input rVpr (lower panel) detected by 8D1 are shown. (**b**) Detection of Vpr in a culture supernatant. Culture supernatants (sup.) of 293FS cells (Invitrogen) transfected with pcDNA3.1 (center lane, "Vec") or pcDNA3.1-*vpr* (right lane, "Vpr") were collected on day 6 after transfection, and the IP-WB analysis was carried out. The rVpr (400 pg/lane) was included in the same blot as a positive control of WB (left lane).

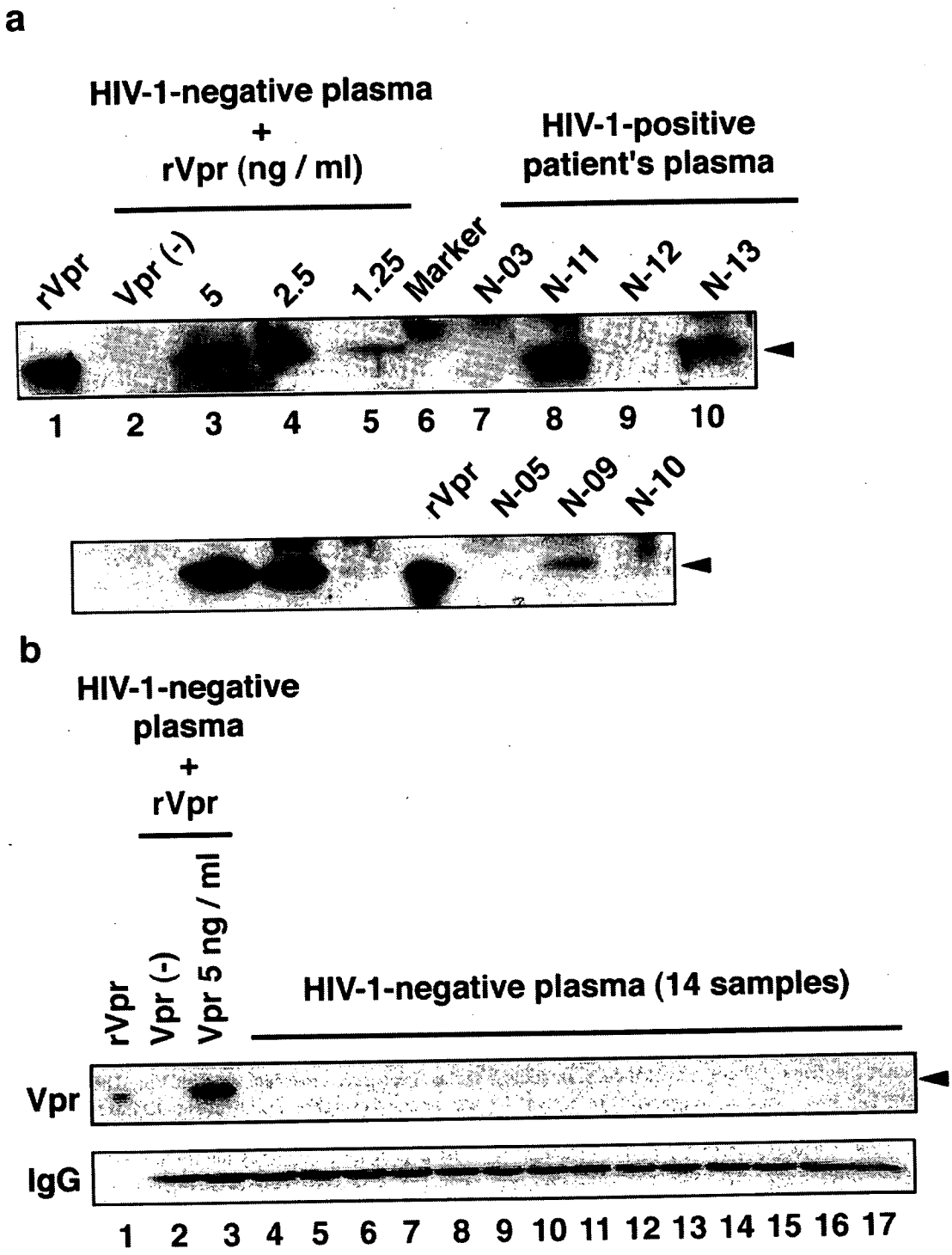

FIG. 1. Detection of Vpr in sera of HIV-1-positive patients. (**a**) Presence of the 14-kDa Vpr protein in HIV-1-positive patients. To semiquantify the Vpr concentration in patient samples, 5, 2.5, and 1.25 ng of standard rVpr (lanes 2–5), which had been measured using ELISA version-1 (see supplementary information 1b; SI-1b), were included. As a positive control for the WB analysis, 1 ng of rVpr (lane 1) was also included. Signals of HIV-1-positive plasma (lanes 7–10) and a molecular marker (lane 6) are shown. (**b**) Representative results of the IP-WB analysis of healthy volunteers. The IP-WB analysis was performed on more than 60 samples from healthy volunteers, and representative results from 14 cases (lanes 4–17) are shown. Note that no signals were detected around 14 kDa. The results for input rVpr (lane 1), no rVpr (lane 2), or 5 ng Vpr (lane 3) added to normal plasma are shown. IgG signals recovered after IP are also shown (lower panel). (**c**) Detection of the 14-kDa Vpr protein in HIV-1-positive patients in the second group. Also in this analysis, 5, 2.5, and 1.25 ng of standard rVpr (lanes 2–5) were included to assess the concentration of Vpr in patient plasma samples.

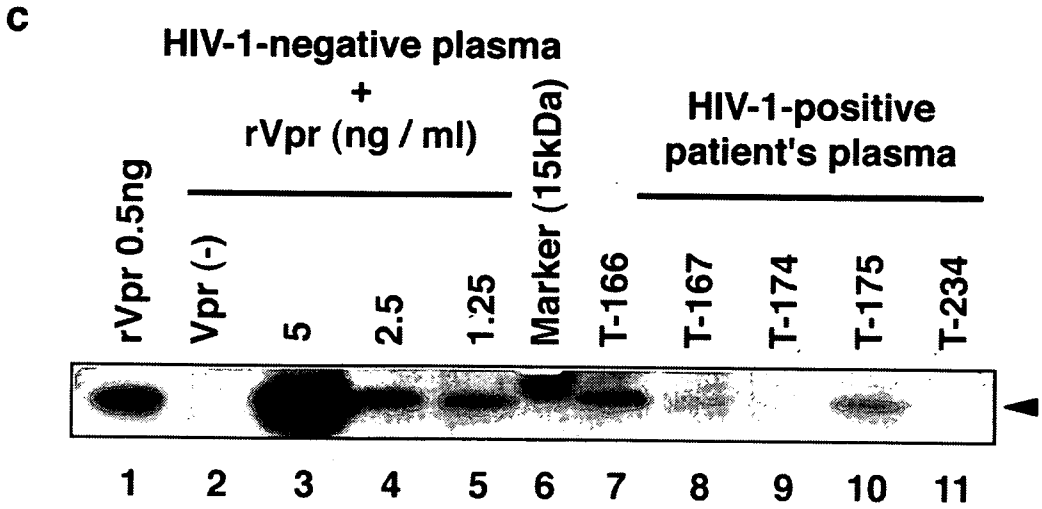

FIG. 1. (*Continued*).

SI-3. Cloning and sequence analysis of *vpr*. DNA covering *vpr* was amplified from the genomic DNA of peripheral blood cells using nested PCR. The primers used were Vpr1F (nt 4713–4733, 5′-GACCCTGACCTAGCAGACCA-3′) and Vpr1R (nt 5298–5318, 5′-CAAACTTGGCAATGAAAGCA-3′) for the first PCR. For the second PCR, Vpr2F (nt. 4854–4875, 5′-CAGTACTTGGCACTAGCAGCA-3′) and Vpr2R (nt 5243–5263, 5′-TAGGCTGACTTCCTGGATGC-3′) were used (GenBank accession number M19921). The first and second rounds of PCR were performed for 30 cycles of 95°C for 30 sec, 62°C for 30 sec, and 72°C for 1 min and for 95°C for 30 sec, 64°C for 30 sec, and 72°C for 45 sec, re-

a

```
NL4-3     1 ATGGAACAAG CCCCAGAAGA CCAAGGGCCA CAGAGGGAGC CATACAATGA ATGGACACTA
Clone-10  1 ---------- ---------- ---------- ---------- ---------- ----------

         61 GAGCTTTTAG AGGAACTTAA     GAGTGA AGCTGTTAGA CATTTTCCTA GGATATGGCT
         61 ---------- ---------- TTAA------ ---------- ---------- ----------

        117 CCATAACTTA GGACAACATA TCTATGAAAC TTACGGGGAT ACTTGGGCAG GAGTGGAAGC
        121 ---------- ---------- ---------- ---------- ---------- ----------

        177 CATAATAAGA ATTCTGCAAC AACTGCTGTT TATCCATTTC AGAATTGGGT GTCGACATAG
        181 ---------- ---------- ---------- ---------- ---------- ----------

        237 CAGAATAGGC GTTACTCGAC AGAGGAGAGC AAGAAATGGA GCCAGTAGAT CCTAG 291nt.
        241 ---------- ---------- ---------- ---------- ---------- ----- 295nt.
```

b

```
NL4-3     MEQAPEDQGPQREPYNEWTLELLEELKSEAVRHFPRIWLHNLGQHIYETYGDTWAGVEAIIRILQQLLFIHFRIGCRHSRIGVTRQRRARNGASRS
Clone-10  ........................N*
Clone-N   ..................................................................Q.....II.............
```

FIG. 2. Sequence analysis of *vprs* and the deduced amino acids of Vpr variants in HIV-1-positive patients. The *vpr* gene was amplified and analyzed, as described in SI-3. (**a**) Nucleotide sequence of clone 10. The nucleotide sequence was compared with that of the prototype NL4-3. Clone 10 has a four-base insertion at nucleotide 81, generating a stop codon within the insert (indicated by the box). Nucleotides that are the same as those in NL4-3 are marked with small bars. (**b**) Amino acid sequences of Vpr variants found in the patients. The amino acids deduced from the obtained sequences and the NL4-3 clone are shown. As described in SI-3a, clone 10 was recognized as a major variant in patient N-10, while clone N was the major variant in patients N-04 and 09.

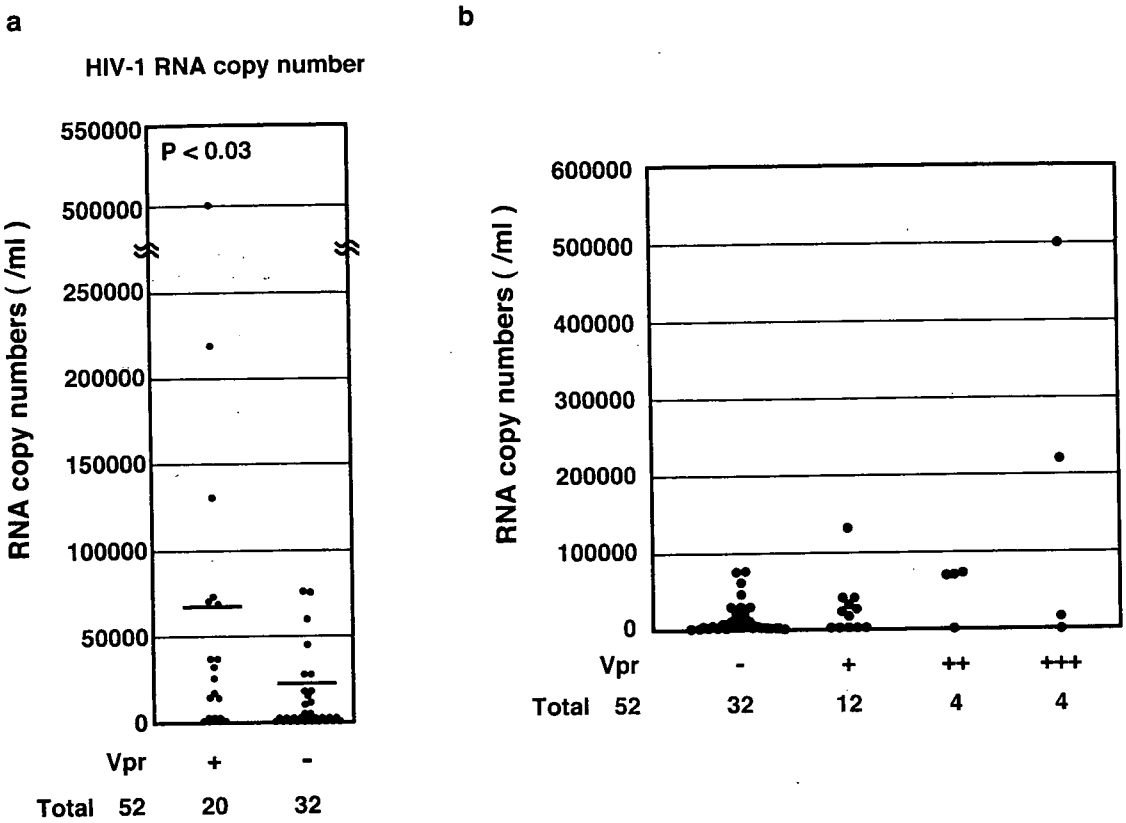

FIG. 3. Correlation between Vpr detection and clinical data. The analyzed cases were divided into Vpr-positive and Vpr-negative groups, and the statistical analysis was done using Student's *t*-test. (**a**). The relationships with the HIV-1 RNA copy number. The bars indicate the mean numbers in each group. The difference for HIV-RNA copy number with Vpr was statistically significant ($p < 0.03$). (**b**) Distribution of Vpr-positive patients according to the concentration of plasma Vpr. Based on the semi-quantitative analysis, patients were divided into four groups: Vpr-negative (−), Vpr-positive with less than 1 ng/ml (+), 1–5 ng/ml (++), and more than 5 ng/ml (+++). Each dot means a patient.

spectively. The PCR products were cloned into pZeroBlunt topo vector (Invitrogen, Carlsbad, CA). Several clones were sequenced for each PCR product.

SI-4. See Table 2.

TABLE 2. FREQUENCY OF *vpr* VARIANTS IN HIV-1 PATIENTS[a]

	vpr *variants*		
Cases	*NL4-3*	*Clone N*	*Clone 10*
N-03	7[b]	—	9
N-04	—	14	—
N-05	2	2	3
N-09	—	7	—
N-10	—	—	5
N-12	4	4	—

[a]PCR products amplified from patient genomic DNA were subcloned into the vector, and several clones were sequenced. The numbers in the table indicate the frequency of clones encountered in the sequence analyses. All 5 clones derived from patient N-10 were clone 10. In patients N-04 and 09, clone N was identified as the major variant; all 14 clones for patient N-04 and all 7 clones for patient N-09 were clone N. Patients N-03 and N-05 each had 2 *vpr* variants.

[b]Number of analyzed clones.

ACKNOWLEDGMENTS

We thank the healthy volunteers and C. Nakai-Murakami for donating peripheral blood and providing technical assistance. We are grateful for samples of HIV-1-positive patients to Drs. C. Kobayashi (National Hospital Organization Chiba Medical Center), I. Sato (National Hospital Organization Sendai Medical Center), H. Hanafusa (Ogikubo Hospital), J. Matsuda (Teikyo University School of Medicine), M. Sakai (University of Occupational and Environmental Health), S. Ikeda (Sasebo Municipal Hospital), and T. Fujii (Hiroshima University School of Medicine). This work was supported by a Grant-in-Aid for Research on Health Sciences focusing on Drug Innovation from the Japan Health Sciences Foundation Research and Research on HIV/AIDS from the Ministry of Health, Labor and Welfare of Japan. Dr. Sun is a research resident supported by the Foundation for AIDS prevention.

REFERENCES

1. Palella FJ, Delaney KM, Moorman AC, Loveless MO, Fuhrer J, Satten GA, *et al.*: Declining morbidity and mortality among patients with advanced human immunodeficiency virus infection. N Engl J Med 1998;338:853–860.

2. Finzi D, Hermankova M, Pierson T, Carruth LM, Buck C, Chaisson RE, *et al.*: Identification of a reservoir for HIV-1 in patients on highly active antiretroviral therapy. Science 1997;278:1295–1300.
3. Folks TM, Justement J, Kinter A, Dinarello CA, Fauci AS: Cytokine-induced expression of HIV-1 in a chronically infected promonocyte cell line. Science 1987; 238:800–802.
4. Koyanagi Y, O'Brien WA, Zhao JQ, Golde DW, Gasson JC, and Chen ISY: Cytokines alter production of HIV-1 from primary mononuclear phagocytes. Science 1988;241:1673–1675.
5. Heinzinger NK, Bukrinsky MI, Haggerty SA, Ragland AM, Kewalramani V, Lee MA, *et al.*: The Vpr protein of human immunodeficiency virus type 1 influences nuclear localization of viral nucleic acids in nondividing host cells. Proc Natl Acad Sci USA 1994;91:7311–7315.
6. Vodicka MA, Koepp DM, Silver PA, and Emerman M: HIV-1 vpr interacts with the nuclear transport pathway to promote macrophage infection. Genes Dev 1998;12:175–185.
7. Jenkins Y, McEntee M, Weis K, and Greene WC: Characterization of HIV-1 vpr nuclear import: Analysis of signals and pathways. J Cell Biol 1998;143:875–885.
8. Levy DN, Refaeli Y, MacGregor RR, and Weiner DB: Serum vpr regulates productive infection and latency of human immunodeficiency virus type 1. Proc Natl Acad Sci USA 1994;91:10873–10877.
9. Levy DN, Refaeli Y, and Weiner DB: Extracellular vpr protein increases cellular permissiveness to human immunodeficiency virus replication and reactivates virus from latency. J Virol 1995;69: 1243–1252.
10. Marzio PD, Choe S, Ebright M, Knoblauch R, and Landau NR: Mutational analysis of cell cycle arrest, nuclear localization, and virion packaging of human immunodeficiency virus type 1 vpr. J Virol 1995;69:7909–7916.
11. Muthumani K, Hwang DS, Desai BM, Zhang D, Dayes N, Green DR, *et al.*: HIV-1 vpr induces apoptosis through caspase 9 in T cells and peripheral mononuclear blood cells. J Biol Chem 2002; 277:37820–37831.
12. Muthumani K, Hwang DS, Choo AY, Mayilvahanan S, Dayes NS, Thieu KP, *et al.*: HIV-1 vpr inhibits the maturation and activation of macrophages and dendritic cells *in vitro*. Int Immunol 2004; 17:103–116.
13. Muthumani K, Choo AY, Zong W-X, Madesh M, Hwang DS, Premkumar A, *et al.*: The HIV-1 vpr and glucocorticoid receptor complex is a gain-of-function interaction that prevents the nuclear localization of PARP-1. Nat Cell Biol 2006;8:170–179.
14. Lum JJ, Cohen OJ, Nie Z, Weaver JG, Gomez TS, Yao X-J, *et al.*: *Vpr* R77Q is associated with long-term nonprogressive HIV infection and impaired induction of apoptosis. J Clin Invest 2003; 111:1547–1554.
15. Rodes B, Toro C, Paxinos E, Poveda E, Martinez-Padial M, Benito JM, *et al.*: Differences in disease progression in a cohort of long-term non-progressors after more than 16 years of HIV-1 infection. AIDS 2004;18:1109–1116.
16. Mologni D, Citterio P, Menzaghi B, Zanone PB, Riva C, Broggini V, *et al.*: Vpr and HIV-1 disease progression: R77Q mutation is associated with long term control of HIV-1 infection in different groups of patients. AIDS 2006;20:567–574.
17. Cavert W, Webb CH, Balfour HH Jr: Alterations in the C-terminal region of HIV-1 accessory gene vpr do not confer clinical advantage to subjects receiving nucleoside antiretroviral therapy. J Infect Dis 2004;20:2181–2184.
18. Chui C, Cheung PK, Brumme CJ, Mo T, Brumme ZL, Montaner JSG, *et al.*: HIV-1 VprR77Q mutation does not influence clinical response of individuals initiating highly active antiretroviral therapy. AIDS Res Hum Retrovir 2006;22:615–618.

Address reprint requests to:
Yukihito Ishizaka
Research Institute
International Medical Center of Japan
1-21-1 Toyama
Shinjuku-ku
Tokyo 162-8655, Japan

E-mail: zakay@ri.imcj.go.jp

Separate elements are required for ligand-dependent and -independent internalization of metastatic potentiator CXCR4

Yuko Futahashi,[1] Jun Komano,[1,4] Emiko Urano,[1] Toru Aoki,[1,2] Makiko Hamatake,[1] Kosuke Miyauchi,[1] Takeshi Yoshida,[3] Yoshio Koyanagi,[3] Zene Matsuda[1] and Naoki Yamamoto[1,2]

[1]AIDS Research Center, National Institute of Infectious Diseases, 1-23-1 Toyama, Shinjuku, Tokyo 162-8640; [2]Department of Molecular Virology, Tokyo Medical and Dental University, 1-5-45, Yushima, Bunkyo-ku, Tokyo 113-8519; [3]Laboratory of Viral Pathogenesis, Institute for Virus Research, Kyoto University, 53 Shougoin-kawahara machi, Sakyou-ku, Kyoto 606-8507, Japan

(Received September 17, 2006/Revised November 3, 2006/Accepted November 11, 2006/Online publication January 19, 2007)

The C-terminal cytoplasmic domain of the metastatic potentiator CXCR4 regulates its function and spatiotemporal expression. However, little is known about the mechanism underlying constitutive internalization of CXCR4 compared to internalization mediated by its ligand, stromal cell-derived factor-1 alpha (SDF-1)/CXCL12. We established a system to analyze the role of the CXCR4 cytoplasmic tail in steady-state internalization using the NP2 cell line, which lacks endogenous CXCR4 and SDF-1 . Deleting more than six amino acids from the C-terminus dramatically reduced constitutive internalization of CXCR4. Alanine substitution mutations revealed that three of those amino acids Ser^{344} Glu^{345} Ser^{346} are essential for efficient steady-state internalization of CXCR4. Mutating Glu^{345} to Asp did not disrupt internalization, suggesting that the steady-state internalization motif is S(E/D)S. When responses to SDF-1 were tested, cells expressing CXCR4 mutants lacking the C-terminal 10, 14, 22, 31 or 44 amino acids did not show downregulation of cell surface CXCR4 or the cell migration induced by SDF-1 . Interestingly, however, we identified two mutants, one with E344A mutation and the other lacking the C-terminal 17 amino acids, that were defective in constitutive internalization but competent in ligand-promoted internalization and cell migration. These data demonstrate that ligand-dependent and -independent internalization is genetically separable and that, between amino acids 336 and 342, there is a negative regulatory element for ligand-promoted internalization. Potential involvement of this novel motif in cancer metastasis and other CXCR4-associated disorders such as warts, hypogammaglobulinemia, infections and myelokathexis (WHIM) syndrome is discussed. (*Cancer Sci* 2007; 98: 373–379)

The chemokine receptor CXCR4 is a class-A G protein-coupled receptor (GPCR; reviewed in [1,2]) and its natural ligand is stromal cell-derived factor-1 alpha (SDF-1)/CXCL12. CXCR4 also serves as the receptor for HIV type 1 (HIV-1). Many cell types express CXCR4, including peripheral blood lymphocytes, monocytes-macrophages, thymocytes, dendritic cells, endothelial cells, epithelium-derived tumor cells, microglial cells, neurons and hematopoietic stem cells. CXCR4 plays multiple biological roles from promoting development of neuronal networks to regulating migration of leukocytes, cerebellar granule cells and hematopoietic stem cells.[3–8] Analysis of knockout mice indicates that the CXCR4/SDF-1 system is essential for maintenance of hematopoiesis and intestinal vascularization.[9,10]

The CXCR4/SDF-1 system also functions in pathological processes, including autoimmune diseases, cancer progression and metastasis, and AIDS caused by HIV-1. Recently, metastasis of breast cancer cells was found to be regulated by the CXCR4/SDF-1 axis.[5] Similarly, other studies have found that metastasis of other malignancies was controlled by the CXCR4/SDF-1 system, including colon carcinoma[11] non-small cell lung cancer[12] and prostate cancer.[13] These observations suggest that the CXCR4/SDF-1 axis is a potential target for metastatic cancer therapy.

Warts, hypogammaglobulinemia, infections and myelokathexis (WHIM) syndrome is a rare combined immunodeficiency characterized by an unusual form of neutropenia. It is reported that the CXCR4 cytoplasmic tail is mutated and often truncated in WHIM syndrome.[14] Thus, determining the biochemical activity of the CXCR4 cytoplasmic tail should facilitate understanding of the pathogenesis of WHIM syndrome as well as suggest ways to control cancer metastasis.

Following SDF-1 binding, CXCR4 is activated, triggering multiple signaling cascades via G or -arrestin 2 (reviewed in[15]). To desensitize activated CXCR4, the G protein-coupled receptor kinase (GRK) is recruited and phosphorylates serine residues on the CXCR4 cytoplasmic tail, thereby inactivating G -mediated signal. Simultaneously, CXCR4 is internalized in a clathrin-dependent manner. -arrestin 2 competes with G for CXCR4 binding and can initiate signal transduction independent from G . -arrestin 2 can also induce clathrin-dependent CXCR4 endocytosis. Thus, cell surface levels of CXCR4 transiently decrease after agonist binding but, several hours later, surface levels of CXCR4 return to normal. Most internalized CXCR4 is transported to lysosomes and degraded, but some internalized CXCR4 is recycled. It is reported that amino acids within the cytoplasmic tail are required for agonist-dependent endocytosis of CXCR4.[16–18]

By contrast, it is unclear how steady-state cell surface levels of CXCR4 are maintained in the absence of SDF-1 . Although cell surface levels of CXCR4 could be regulated at the transcriptional level, it is likely that primary regulation occurs post-translationally. Given that the cell surface levels of CXCR4 are positively correlated with cancer cells' ability to metastasize,[5,19] understanding the post-translational behavior of CXCR4 is likely to shed light on metastatic processes. Historically, cells expressing endogenous CXCR4 have been used for analysis of CXCR4 trafficking. However, as is the case with many G protein-coupled receptors (GPCR), CXCR4 trafficking is influenced by spontaneous oligomerization in the absence of ligand.[20–22] Thus, previous observations might not correctly model phenotypes seen in CXCR4 mutants.

In the present study, we analyzed the contribution of the cytoplasmic tail to the post-translational trafficking of CXCR4 in a cell line lacking both endogenous CXCR4 and SDF-1 . Using genetic approaches, we identified two amino acid motifs within the CXCR4 cytoplasmic tail; one that positively regulates

[4]To whom correspondence should be addressed. E-mail:ajkomano@nih.go.jp

doi: 10.1111/j.1349-7006.2007.00388.x

spontaneous ligand-independent internalization and the other that negatively regulates ligand-dependent CXCR4 internalization.

Materials and methods

Cells. The glioblastoma cell line NP2, human embryonic kidney (HEK) 293T, and HeLa, cells were maintained in RPMI-1640 (Sigma, Tokyo, Japan) supplemented with 10% FBS (Japan Bioserum, Tokyo, Japan), penicillin and streptomycin (Invitrogen, Tokyo, Japan). All cell lines were incubated at 37 C in the humidified 5% CO_2 atmosphere.

Plasmids. Full-length CXCR4 cDNA was amplified from a plasmid kindly provided by Dr Shioda[23] using the following primers: sense, 5 -ACCGGTGCCACCATGGAGGGGATCAGTATATACACTTCAG-3 , and antisense, 5 -AGATCTCGCTGGAGTGAAAACTTGAAGACTCAGACTC-3 . CXCR4 lacking the cytoplasmic tail (d-44) was amplified using the same sense primer and the antisense primer, 5 -AGATCTTGGCTCCAAGGAAAGCATAGAGGATGGG-3 . Polymerase chain reaction (PCR) fragments were cloned into the *Age* I-*Bgl* II sites of pEGFP-C2 (Clontech, Palo Alto, CA, USA) to create pCXCR4 FL and pCXCR4 d-44, respectively. To construct pCXCR4 FL- and d-44-GFP, the *Sna* BI-*Bgl* II fragments from pCXCR4 FL and d-44 were cloned into the *Sna* BI-*Bgl* II sites of pEGFP-N2, respectively (Clontech). To construct pCXCR4 FL- and d-44-GFP flag, the *Sna* BI-*Bgl* II fragments from pCXCR4 FL and d-44 were cloned into the *Sna* BI-*Bgl* II sites of pEGFP-flag in which the following annealed oligonucleotides had been inserted into the *Bsr* GI site of pEGFP-N2: forward, 5 -GTACGACTACAAAGACGATGACGACTATAAGTAAGC-3 , and reverse, 5 -GGCCGCTTACTTATAGTCGTCATCGTCTTTGTAGTC-3 . To construct pCMMP CXCR4 FL- and d-44-GFP, pCXCR4 FL- and d-44-GFP were digested with *Not* I, blunted using T4 DNA polymerase, and further digested with *Age* I. The Age *I*-blunted *Not* I fragments of both constructs were cloned into the pCMMP eGFP plasmid that had been digested with *Bam* HI, blunted with T4 DNA polymerase, and digested with *Age* I. pCMMP CXCR4 FL- and d-44-GFP-flag were constructed using the same strategy. CXCR4 deletion and point mutants were PCR-amplified using the sense primer 5 -ACCGGTGCCACCATGGAGGGGATCAGTGTGAAAACTTGAAGACTCAGACTC-3 and the following reverse primers: d-6, 5 -AAGCTTGAGCTCGAGATCTCAGACTCAGACTCAGTGGAAAC-3 ; d-10, 5 -AAGCTTGAGCTCGAGATCTCAGTGGAAACAGATGAATGTCC-3 ; d-14, 5 -AAGCTTGAGCTCGAGATCTCTGAATGTCCACCTCGCTTTCC-3 ; d-17, 5 -AAGCTTGAGCTCGAGATCTCACCTCGCTTTCCTTTGG-3 ; d-22, 5 -AAGCTTGAGCTCGAGATCTCGGAGAGGATCTTGAGGCTGGACC-3 ; d-31, 5 -AAGCTTGAGCTCGAGATCTCGCTCACAGAGGTGAGTGCGTGC-3 ; E343A, 5 -CGAGATCTCGCTGGAGTGAAAACTTGAAGACTCAGACGCAGTGGAAACAGATGAATGTC-3 ; S344A, 5 -CGAGATCTCGCTGGAGTGAAAACTTGAAGACTCAGCCTCAGTGGAAACAGATGAATGTC-3 ; E345A, 5 -CGAGATCTCGCTGGAGTGAAAACTTGAAGACGCAGACTCAGTGGAAACAGATGAATGTC-3 ; S346A, 5 -CGAGATCTCGCTGGAGTGAAAACTTGAAGCCTCAGACTCAGTGGAAACAGATGAATGTC-3 S347E, 5 -CGAGATCTCGCTGGAGTGAAAACTTTCAGACTCAGACTCAGTGGAAACAGATGAATGTC-3 ; H350E, 5 -CGAGATCTCGCTGGACTCAAAACTTGAAGACTCAGACTCAGTGGAAACAGATGAATGTC-3 ; S347E/H350E, 5 -CGAGATCTCGCTGGACTCAAAACTTTCAGACTCAGACTCAGTGGAAACAGATGAATGTC-3 ; and E343/345D, 5 -CGAGATCTCGCTGGAGTGAAAACTTGAAGAGTCAGAGTCAGTGGAAACAGATGAATGTC-3 . The PCR fragments were cloned into the *Age* I-*Bgl* II sites of pCMMP CXCR4 FL-GFP-flag, replacing wild-type with mutant CXCR4. Protein expression of each mutant in 293T cells was verified by Western blot analysis.

Immunoblotting. Immunoblotting was performed as described.[24,25] The primary antibody was anti-green fluorescent protein (GFP) polyclonal antibody (Beckton Dickinson, San Jose, CA, USA). The secondary probe was EnVision+ (Dako, Glostrup, Denmark). Signals were visualized with an LAS3000 imager (Fuji Film, Tokyo, Japan) after treating the membranes with the Lumi-Light Western Blotting Substrate (Roche Diagnostics GmbH, Mannheim, Germany).

Flow cytometry. Cells were labeled with anti-CXCR4 antibodies recognizing the N-terminus conjugated with R-phycoerythrin (PE; 2B11, BD Pharmingen, San Diego, CA) or recognizing the second extracellular loop (12G5) conjugated with either PE or PE-Cy5 (Beckton Dickinson) for 30 min at 4 C. Cells were washed once with phosphate-buffered saline (PBS) supplemented with 1% FBS and analyzed by FACS Aria (Beckton Dickinson). To isolate GFP-expressing NP2 cells, cells were infected with murine leukemia virus (MLV)-based retroviral vectors as described.[25] Cells exhibiting similar green fluorescence intensities were gated and sorted by FACS Aria. Efficiency of internalization was measured by comparing mean fluorescence intensities for cell surface CXCR4 detected by a PE-labeled 2B11 monoclonal antibody before and after SDF-1 treatment (200 ng/mL, Peprotech EC, London, UK).

Microscopic analysis and imaging of cells. To judge a phenotype of a CXCR4 mutant, three independent scientists investigated the mutant cell phenotype under a fluorescent microscope (Olympus, Tokyo, Japan). Each scientist investigated more than 1000 cells for each mutant. More than 99% of cells of a mutant fell in the indicated phenotypic category. These phenotypes were unchanged for more than a year of continuous cultivation in tissue culture. For imaging, NP2 cells were grown on glass plates for more than 24 h, fixed in 4% formaldehyde in PBS for 5 min, stained with Hoechst 33258, mounted (Vectorshield, Vector Laboratories, Burlingame, CA, USA), and imaged using a confocal microscope META 510 (Carl Zeiss, Tokyo, Japan). A representative cell for each CXCR4 mutant carrying a wide cytoplasm was chosen such that the spatial resolution was high. The focal plane just above the glass surface was scanned with an optical thickness of approximately 1 m. For the imaging of subcellular compartments, cells were incubated with either BODIPY TR ceramid, ER-Tracker Blue-White DPX, or Lysotracker Red DND-99 (Invitrogen) according to the manufacturer's protocol and imaged without fixation. Image brightness and contrast were processed by META510 software (Carl Zeiss). Unless noted, cells were imaged at ×630 magnification, the GFP signal was displayed in green, and Hoechst 33258-stained nuclei were blue. To visualize ligand-induced internalization, cells were treated with 200 ng/mL SDF-1 before fixation. The live cell imaging was performed using Leica DFC350FX system and the images were processed by FW4000 software (Leica Microsystems, Tokyo, Japan). Cells were plated on the glass-bottomed dish (Matsunami glass, Kishiwada, Japan) and incubated at 37 C in the humidified 5% CO_2 atmosphere during the monitoring.

Cell migration assay. Cell migration was measured using an HTS FluoroBlok Multiwell Insert System (8.0 m pore size, BD Falcon) according to the manufacturer's protocol. For stimulation assays, cells were incubated without serum overnight before SDF-1 treatment (200 ng/mL). Cells were allowed to migrate overnight.

Statistical analysis. Significance of differences were determined by a Student's *t*-test. *P*-values less than 0.05 were considered significant.

RESULTS

Deleting 10 amino acids from the carboxyl end of CXCR4 alters the efficiency of constitutive internalization. Previous studies indicated that the cytoplasmic tail of CXCR4 amino acids 308–352 plays

doi: 10.1111/j.1349-7006.2007.00388.x

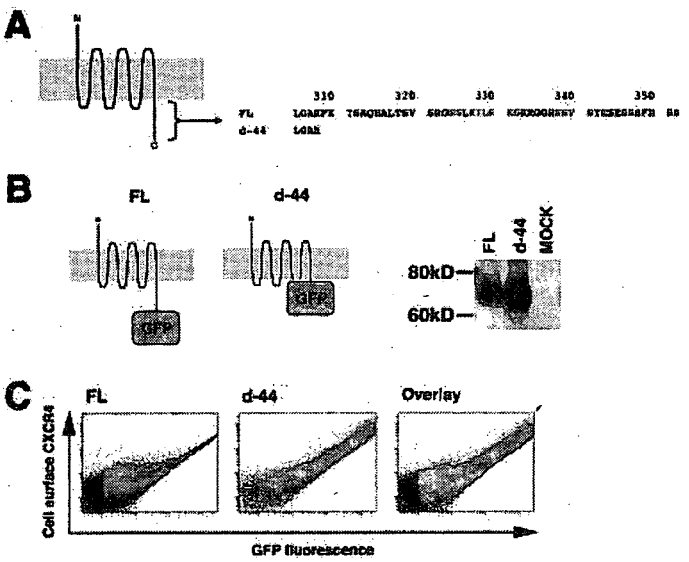

Fig. 1. The effect of stromal cell-derived factor-1 alpha (SDF-1) treatment on NP2 cells expressing CXCR4 mutants. (a) Cells expressing d-17 were treated with SDF-1 , incubated at 37 C for the indicated times, fixed and imaged. The blue signal represents the Hoechst-stained nucleus. (Original magnification, ×630; bar, 10 m). (b) FACS analysis to measure internalization efficiency of cell surface CXCR4 and mutant forms 2 h after SDF-1 exposure. The average and standard deviation from the indicated number of independent experiments are shown. Asterisks represent statistically significant difference from the FL levels ($P < 0.01$). (c) Cell migration assay to assess response of cells expressing CXCR4 and mutants to SDF-1 . The number of migrated cells in three to six randomly selected fields was counted and the average and standard deviation were calculated. ( ) number of migrated cells in the absence of ligand; ( ) migration in the presence of ligand. (*) statistically significant differences in the number of migrated cells between SDF-1 -untreated and -treated cells ($P < 0.01$).

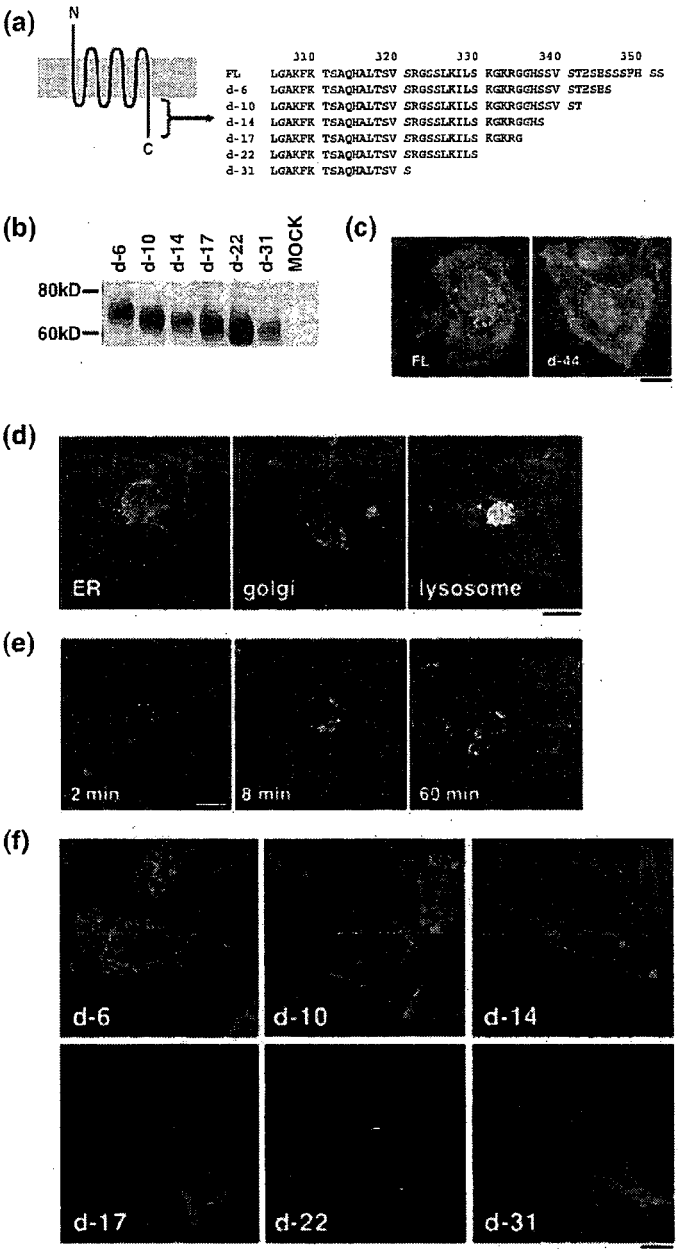

Fig. 2. Expression profiles of CXCR4 and a mutant with cytoplasmic tail deletion. (a) Schematic representation of CXCR4. The N-terminus CXCR4 is exposed in the extracellular space and the C-terminus is intracellular. Gray represents the lipid bilayer. The amino acid sequence of the cytoplasmic tail is shown. Residues in red are required for ligand-induced endocytosis. The CXCR4 d-44 mutant lacks amino acid 309–351. (b) Schematic representation and Western blot of FL and d-44 constructs. (c) Flow cytometry profiles of FL and d-44 expressed in 293T cells. The horizontal axis represents green fluorescence intensity indicative of green fluorescent protein (GFP)-tagged CXCR4 protein levels, and the vertical axis is PE-Cy5 fluorescence intensity, reflecting cell surface CXCR4 detected by the anti-CXCR4 antibody. GFP-positive cells expressing FL are colored in red (left) and those expressing d-44 in green (middle). The expressional differences between FL and d-44 is highlighted on the overlay plot (right).

a critical role in ligand-dependent internalization (Fig. 1a). Also, it has been shown in transfected cells that cell surface levels of CXCR4 lacking the cytoplasmic tail (equivalent to the d-44 mutant here) are higher than those of the full length, wild-type protein (hereafter designated FL), suggesting that the cytoplasmic tail of CXCR4 regulates steady-state internalization.[26,27] To confirm this, we constructed expression plasmids of CXCR4 FL and d-44 fused to GFP or GFP-FLAG at the C-terminus. Previous studies and data reported here indicated that CXCR4 function is not affected by this modification.[28] The expression of each construct was verified by Western blot analysis (Fig. 1b). Single cell-based quantitative analyzes revealed that the ratio of cell surface levels to the total amount of CXCR4 FL (Fig. 1c, left) was consistently lower than that of d-44 (Fig. 1c, middle) at any expression levels (Fig. 1c, right for the comparison). These data supported previous findings and demonstrate that constitutive internalization occurs at any level of CXCR4 expression.

To further examine the contribution of the cytoplasmic tail to post-translational trafficking of CXCR4, we devised a system utilizing the human NP2 glioma line: NP2 cells are flat and exhibit a large cytoplasmic space such that intracellular compartments can be well resolved under the microscope. NP2 cells also lack endogenous CXCR4[29] and SDF-1 (data not shown), both of which could potentially affect distribution of transduced CXCR4. However, NP2 cells are capable of appropriate signaling in response to CXCR4/SDF-1 interaction. We generated a series of CXCR4 deletion mutants lacking the cytoplasmic tail (Fig. 2a) and transduced them into NP2 cells using MLV vectors. Cells bearing similar green fluorescence intensities were collected by FACS sorter. The expression of each mutant was verified by Western blot analysis (Fig. 2b). Microscopic observations revealed that cells expressing FL were bordered by green fluorescence, and significant green fluorescence was detected in vesicular compartments of varying diameters lying close to the nucleus surrounding the nucleus (hereafter designated the FL phenotype, Fig. 2c, left). Vesicles around the nucleus were

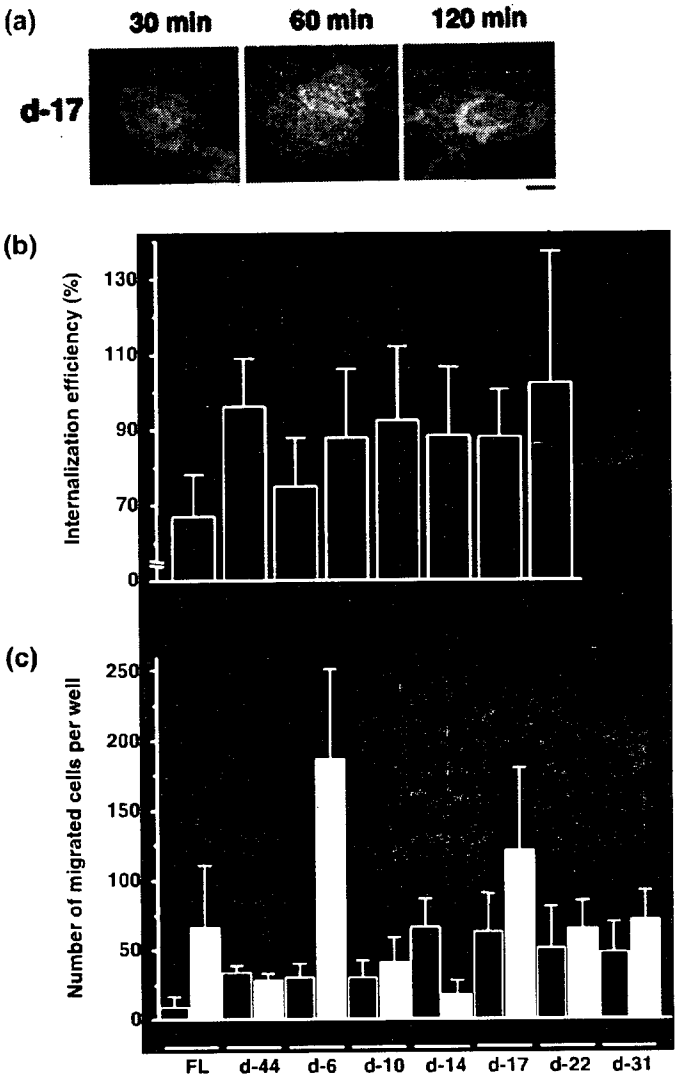

Fig. 3. Identification of the amino acids required for steady-state CXCR4 internalization. (a) Amino acid sequences of the cytoplasmic tail of FL and deletion mutants. Residues in red are required for ligand-induced endocytosis. (b) The protein expression of each mutant in 293T cells was verified by Western blot analysis. (c) Confocal micrographs of NP2 cells expressing FL and d-44 mutant proteins. The blue signal represents the Hoechst-stained nucleus. (Original magnification, ×630; bar, 10 m.) (d) Confocal micrographs showing NP2 cells expressing CXCR4 FL stained with ER, Golgi, or lysosome organella markers. The organella marker signal is shown in red, the GFP signal is in green. The pixels that both red and green signals co-localized are shown in yellow. (Original magnification, ×630; bar, 10 m.) (e) CXCR4 FL trafficking in the absence of SDF-1 in NP2 cells. Cell surface CXCR4 FL was labeled with an antibody conjugated with PE-Cy5 (red), incubated at 37 C for the indicated times, fixed and imaged. (Original magnification, ×630; bar, 10 m.) (f) Confocal micrographs of NP2 cells expressing FL and mutant proteins. The intracellular vesicular green fluorescence reflecting steady-state internalization can be seen in the d-6 mutant. The blue signal represents the Hoechst-stained nucleus. (Original magnification, ×630; bar, 10 m.)

mostly lysosomes, as demonstrated by fluorescent organella marker analyses in which cells expressing CXCR4 FL-GFP stained with the lysosomal marker yielded a substantial amount of co-localization signal. On the other hand, only a mall amount of co-localization signal was detected when the ER or Golgi markers were used (Fig. 2d), consistent with our biochemical fractionation (unpublished data) and previous publications.[16,27,28,30] The active constitutive internalization was visualized by labeling cell surface CXCR4 by PE-Cy5-conjugated monoclonal antibody followed by fluorescence imaging after cells were incubated at 37 C (Fig. 2e). The live cell imaging revealed that internalizing GFP-positive vesicles trafficked at an average velocity of 4.7 mm/h ($n = 15$), which is within the range of clathrin-dependent vesicular transport (2–20 mm/h), not that of caveolin-dependent vesicular transport (25–170 mm/h).[31–35] These data suggest that the FL is constitutively internalized from the cell surface to the cytoplasmic compartment. In sharp contrast, most green fluorescent signals from d-44 mutant-expressing cells were detected at the cell surface, and only a few small GFP-positive vesicles were seen in the cytoplasm near the nucleus (hereafter designated the d-44 phenotype, Fig. 2c, right). Similar observations were made in d-10, d-14, d-17, d-22 and d-31 mutant-expressing cells (Fig. 2f). The d-6 construct displayed a phenotype similar to FL, although the intracellular GFP signal was less prominent (Fig. 2c). Similar results were obtained in HeLa and 293 cells (data not shown). These data suggest that wild-type CXCR4 was trafficked to the plasma membrane but was internalized spontaneously. Thus, steady-state internalization appeared to be regulated by amino acids located between d-6 and d-10 (e.g. amino acids 343–346).

Steady-state and SDF-1 -induced CXCR4 internalization is genetically separable. Next, we investigated distribution of CXCR4 protein and cell migration after SDF-1 treatment. Confocal analysis showed that after SDF-1 exposure, cells expressing FL, d-6 and d-17 mutants showed GFP signals in intracellular compartments, which were enhanced 60 min after SDF-1 treatment, an effect most clearly shown in d-17-expressing cells (Fig. 3a). GFP signals from intracellular vesicles gradually disappeared 1–2 h after exposure to ligand. Such redistribution of GFP signals was not observed in cells expressing d-10, d-14, d-22, d-31 and d-44 (data not shown). Cell surface levels of CXCR4 before and after SDF-1 treatment were measured by FACS analysis undertaken with an antibody directed against the CXCR4 N-terminus, because that antibody did not interfere with ligand–receptor interaction (Fig. 3b). The downregulation of cell surface levels of FL 2 h after ligand exposure was 67.1 11.1%, whereas that of d-44 was 96.3 12.3% (average and standard deviation from 12 and 10 independent experiments, respectively), consistent with previous reports.[17,27,28] Ligand-induced downregulation of d-6 was 74.9 12.9% ($n = 8$), similar to FL levels. Ligand-induced internalization was significantly less efficient in cells expressing d-10, d-14, d-17, d-22, d-31 and d-44 mutants when compared with FL ($P < 0.001$). Although the d-17 mutant supported ligand-facilitated internalization, as evidenced by microscopic observation, cell surface levels remained unchanged (Fig. 3a,b). This may be due in part to rapid recruitment of newly synthesized d-17 to the cell surface.

Next, we examined cells expressing CXCR4 mutants in response to SDF-1 . Migration results from intracellular signaling initiated by SDF-1 /CXCR4 interaction. Induction of cell migration by SDF-1 in cells expressing FL was 7.2-fold that of untreated cells ($P < 0.05$). In contrast, migration of cells expressing d-44 in response to SDF-1 was undetectable. These data are in agreement with a previous report.[26] The d-6 mutant, which is internalized upon SDF-1 treatment, supported ligand-promoted cell migration by 6.1-fold ($P < 0.01$) relative to untreated cells, similar to FL. Other deletion mutants tested did not display enhanced cell migration following ligand treatment, except for d-17, which showed modestly enhanced (1.9-fold) migration relative to untreated cells, which was not statistically significant. When basal migratory activities were compared, removal of six or more amino acids from the cytoplasmic tail appeared to potentiate migration in the absence of ligand (open bars, Fig. 3c). These data suggest that constitutive internalization is regulated independently of ligand-facilitated internalization.

Identification of CXCR4 S(E/D)S as a ligand-independent internalization motif. The above data indicated that the carboxy-terminal four

doi: 10.1111/j.1349-7006.2007.00388.x